

1-1-2014

Human gingival mesenchymal stem cells and self-assembling peptide PuraMatrix(TM) scaffold for bone formation

Don Do

Nova Southeastern University

This document is a product of extensive research conducted at the Nova Southeastern University [College of Dental Medicine](#). For more information on research and degree programs at the NSU College of Dental Medicine, please click [here](#).

Follow this and additional works at: https://nsuworks.nova.edu/hpd_cdm_stuetd

Part of the [Dentistry Commons](#)

Share Feedback About This Item

NSUWorks Citation

Don Do. 2014. *Human gingival mesenchymal stem cells and self-assembling peptide PuraMatrix(TM) scaffold for bone formation*. Master's thesis. Nova Southeastern University. Retrieved from NSUWorks, College of Dental Medicine. (29)
https://nsuworks.nova.edu/hpd_cdm_stuetd/29.

This Thesis is brought to you by the College of Dental Medicine at NSUWorks. It has been accepted for inclusion in College of Dental Medicine Student Theses, Dissertations and Capstones by an authorized administrator of NSUWorks. For more information, please contact nsuworks@nova.edu.

HUMAN GINGIVAL MESENCHYMAL STEM CELLS AND SELF-ASSEMBLING
PEPTIDE PURAMATRIX™ SCAFFOLD FOR BONE FORMATION

Don Dinh Do

A Thesis Presented to the Faculty of the College of Dental Medicine of Nova
Southeastern University in Partial Fulfillment of the Requirements for the Degree of
MASTER OF SCIENCE

July 2014

© Copyright by Don Dinh Do July 2014

All Rights Reserved

HUMAN GINGIVAL MESENCHYMAL STEM CELLS AND SELF-ASSEMBLING
PEPTIDE PURAMATRIX™ SCAFFOLD FOR BONE FORMATION

By

Don Dinh Do

A thesis submitted to the College of Dental Medicine of Nova Southeastern University in
partial fulfillment of the requirements for the degree of

MASTER OF SCIENCE

Pediatric Dentistry College of Dental Medicine Nova Southeastern University

July 2014

Approved as to style and content by:

APPROVED BY: _____

Committee Chair Umadevi Kandalam Ph.D, M.S. Date

APPROVED BY: _____

Committee Member Romer Ocanto D.D.S, M.S., Me.D. Date

APPROVED BY: _____

Committee Member Alejandro Ibarra D.D.S, M.S.D Date

APPROVED BY: _____

Committee Member George White D.D.S, Ph.D. Date

APPROVED BY: _____

Dean Linda C. Niessen, D.M.D, M.P.H. Date



STUDENT NAME: Don D. Do, D.D.S

STUDENT E-MAIL ADDRESS: dd1145@nova.edu

STUDENT TELEPHONE NUMBER: (714) 716-6379

COURSE DESCRIPTION: Master of Science in Dentistry with specialization in postgraduate Pediatric Dentistry

TITLE OF SUBMISSION: Human Gingival Mesenchymal Stem Cells and Self-Assembling Peptide PuraMatrix™ Scaffold for Bone Formation

DATE SUBMITTED: July 2014

I certify that I am the sole author of this thesis, and that any assistance I received in its preparation has been fully acknowledged and disclosed in the thesis. I have cited any sources from which I used ideas, data, or words, and labeled as quotations any directly quoted phrases or passages, as well as providing proper documentation and citations. This thesis was prepared by me, specifically for the M.S. degree and for this assignment.

STUDENT SIGNATURE: _____
Don D. Do D.D.S. Date

DEDICATION

I dedicate this dissertation to my loving family and friends. A special feeling of gratitude to my parents, Lam Dinh Do and Van Thi Vo, whose encouragement and unconditional love have supported me throughout every stage of my life. Also, I dedicate this to my love, Kimthy Tran, and my best friend, Peter Chong, for motivating me and always believing in my abilities.

ACKNOWLEDGEMENTS

First, I would like to thank my advisor, Dr. Umadevi Kandalam, for her incredible mentorship and guidance throughout the development of this research. Through her dedication to her postgraduate residents, craniofacial research fellows, predoctoral students, undergraduate students, and laboratory collaborators, she creates learning and working atmosphere of high morale, motivation, and harmony.

Secondly, I would like to thank the members of my Masters Committee for their inspiration. I would like to thank Dr. Romer Ocanto for sharing his knowledge in research and introducing me to higher level of academia. I would like to thank Dr. Alejandro Ibarra for his support and sharing his enthusiasm for this *in vivo* study. I would like to thank Dr. George White for the brilliance in his comments and suggestions enhancing this study.

Lastly, I want to express many thanks to everyone that participated in this research. I wish to express my appreciation to Dr. Velez for her expertise in histology, Mrs. Debbie Stiles for her assistance with the CT scans, Dr. Nora Alamer, Dr. Casey Lynn, and research collaborators at University of Miami. The biggest thanks go to Dr. Reem Almashat for her support and words of encouragement throughout this process from start to finish.

ABSTRACT

Human Gingival Mesenchymal Stem Cells and Self-Assembling Peptide PuraMatrix™ Scaffold for Bone Formation

June 2014

Don Dinh Do

M.S., NOVA Southeastern University College of Dental Medicine

D.D.S., New York University College of Dentistry

Directed by: Professor Umadevi Kandalam, Pediatric Dentistry, NSU College of Dental Medicine

Purpose: Among various craniofacial defects, cleft palate is the most common congenital birth defect. Reconstruction of bony parts in the hard palate is important to preserve normal craniofacial growth. Autologous bone grafting is associated with donor site morbidity, extensive healing time, and scar formation. Tissue engineering techniques remain a viable option for the repair and reconstruction of bone. In this study, human gingiva-derived mesenchymal stem cells (HGMSCs) were used in combination with a self-assembled injectable hydrogel scaffold PuraMatrix™ for their ability to regenerate bone. The ability of bone formation of the cell-gel combination was assessed in rat ectopic bone formation system. Methods: HGMSCs were cultured under standard culture conditions. Cells obtained from 3rd passage were encapsulated in 0.5% PuraMatrix™ gel. The cell proliferation was monitored at day 1, 3, 5, and 7 using Live/Dead cell assay. Osteogenesis was determined by assessing matrix mineralization at 4 weeks. The cell-gel constructs were implanted in subcutaneous pockets of 4-week-old Sprague Dawley rats. The bone formation was followed at 2 and 4 weeks using histological and computed tomography scans. Results: Cells encapsulated in PuraMatrix™ were viable and cell growth was observed from day 3. Matrix mineralization was observed at 4 weeks in cell-gel inserts. The bone formation was

observed after 4 weeks of implantation. Conclusion: The self-assembled injectable PuraMatrix™ scaffold in combination with HGMSCs can support bone tissue growth in 4 weeks.

TABLE OF CONTENTS

Dedications.....	v
Acknowledgements.....	vi
Abstract.....	vii
Table of Contents.....	ix
List of Figures.....	xiii
List of Tables.....	xv
List of Abbreviations.....	xvi

CHAPTER 1: INTRODUCTION

1.1 Background.....	1
1.2 Current surgical methods.....	2
1.3 Complications.....	3
1.4 Paradigm shift.....	3
1.5 Tissue engineering.....	3
1.6 Cells.....	4
1.7 Signals.....	4
1.8 Scaffolds.....	4
1.9 Bone tissue engineering.....	5
1.10 Human Gingival Derived Mesenchymal Stem Cells.....	5
1.11 Injectable Hydrogels.....	6
1.12 PuraMatrix™.....	7
1.13 Objective.....	9
1.14 Specific Aims and Hypothesis.....	9

1.14.1 Specific Aim 1: Characterizing cell-gel constructs of HGMSCs and PuraMatrix™	9
1.14.2 Specific Aim 2: Evaluate bone formation capacity of HGMSCS embedded in PuraMatrix™ hydrogel	10
1.14.3 Hypothesis	10
1.15 Location of study	11

CHAPTER 2: MATERIALS AND METHODS

2.1 Overall Study Design	12
2.1.1 Specific Aim 1: Characterizing cell-gel constructs of HGMSCs and PuraMatrix™	12
2.1.2 Specific Aim 2: Evaluate bone formation capacity of HGMSCS embedded in PuraMatrix™ hydrogel	12
2.2 Materials	14
2.3 Isolation of MSC from gingival tissue	15
2.4 Cell Culture	15
2.5 Characterization of HGMSCs by surface markers by flow cytometry method	16
2.6 HGMSCs encapsulation and culture in Puramatrix™ (cell-gel constructs 3D culture) scaffold	16
2.7 Scanning Electronic Microscopy Studies	17
2.8 Cell viability	18
2.8.1 WST Assay	18
2.9.8 Live Dead Cell Assay	19
2.9 <i>In vitro</i> confirmation of osteogenic differentiation	20

2.9.1 Gene expression assay (RT-PCR)	21
2.9.2 Matrix mineralization using Alizarin Red Stain.....	22
2.10 <i>In vivo</i> study.....	22
2.10.1 Animal subjects.....	22
2.10.2 Anesthesia.....	23
2.10.3 Cell culture and differentiation	24
2.10.4 Subcutaneous implantation/ectopic bone formation.....	24
2.10.5 Post-operative Care.....	26
2.11 Bone analysis.....	26
2.11.1 CT scans.....	26
2.11.2 Histological analysis.....	27
2.12 Statistical analysis.....	28

CHAPTER 3: RESULTS

3.1 Isolation and culture of human gingival cells.....	29
3.2 Flow Cytometry analysis.....	29
3.3 Cell growth in PuraMatrix™ (cell –gel constructs 3D model).....	30
3.3.1 Light microscopic observation.....	31
3.4 Scanning Electronic Microscopy Studies.....	32
3.5 Cell growth in Puramatrix™ (cell –gel constructs 3D model)	34
3.5.1 WST assay.....	34
3.5.2 Live Dead Cell Assay.....	34
3.6 Osteogenic Differentiation.....	35
3.6.1 Expression of osteogenic marker genes.....	35

3.6.2 Matrix mineralization using Alizarin Red Stain.....	36
3.7 HGMSCs seeded PuraMatrix™ induces <i>in vivo</i> bone formation.....	37
3.7.1 CT scans.....	37
3.7.2 Histological Analysis.....	41
<u>Chapter 4: Discussion and Conclusions</u>	
4.1	
Discussion.....	44
4.2 Conclusion.....	51
Appendix.....	53
Bibliography.....	55

List of Figures

Figure 1.1: Cleft palate photograph.....	1
Figure 1.5: Tissue engineering concept.....	4
Figure 1.10: Mesenchymal Stem Cells.....	7
Figure 1.11: Injectable peptide hydrogel scaffold.....	7
Figure 1.12A: PuraMatrix™ structure.....	9
Figure 1.12B: PuraMatrix™ gel.....	9
Figure 2.1.1: Specific Aim 1 flow chart.....	13
Figure 2.1.2: Specific Aim 2 flow chart.....	14
Figure 2.5: Flow cytometry: BD FACSAria IIIu.....	16
Figure 2.7: Scanning Electron Microscope: FEI Quanta 200.....	18
Figure 2.8.1: WST Assay.....	19
Figure 2.8.2: Live/Dead Cell Assay: Olympus IX51.....	20
Figure 2.10.1: Sprague Dawley rat.....	23
Figure 2.10.4A: Injectable group diagram and surgical photograph.....	25
Figure 2.10.4B: Preformed group diagram and surgical photograph.....	25
Figure 2.11.1: i-CAT.....	27
Figure 3.1: Isolated HGMSCs.....	29
Figure 3.2: Flow cytometry analysis.....	30
Figure 3.3.1A: Light microscopy of HGMSCs at day 1 and 3.....	31
Figure 3.3.1B: Light microscopy of HGMSCs at day 5.....	31
Figure 3.3.1C: Light microscopy of HGMSCs at day 7.....	32

Figure 3.5: SEM of PuraMatrix™ and HGMSCs seeded PuraMatrix™	33
Figure 3.5.1: WST Assay graph.....	34
Figure 3.5.2: Live/Dead Cell Assay at day 1, 3, 5, and 7.....	35
Figure 3.6.1: RT-PCR Assay.....	36
Figure 3.6.2: Alizarin Red Stains of monolayer and encapsulated HGMSCs.....	37
Figure 3.7.1A: CT scans of control and week 2.....	38
Figure 3.7.1B: CT scans of week 4.....	38
Figure 3.7.1C: CT scans of week 4.....	39
Figure 3.7.2A: Recovery of scaffold implant.....	42
Figure 3.7.2B: Histological slides of control sites.....	42
Figure 3.7.2C: Histological slides of experimental site.....	43
Figure 3.7.2D: Histological slides of experiment sites.....	43

List of Tables

Table 1.2: Available surgical procedures.....	1
Table 2.9.1: Specific primers.....	21
Table 2.10.1: Veterinary anesthetic concentration.....	24
Table 3.7.1A: Radiopacity findings.	40
Table 3.7.1B: Percentage of radiopacity from CT scans.....	41
Table 3.7.2A: Bone Formation Findings	44
Table 3.7.2B: Percentage of bone formation from histological analysis.....	44
Table 4.1: Literature review of current PuraMatrix™ studies.....	47

List of Abbreviations

BMMSCs	Bone marrow derived mesenchymal stem cells
CM	Complete medium
CT	Computed Tomography
CNCC	Cranial neural crest cells
DEPC	Dental pulp derived stem cells
DMEM	Dulbecco's modified eagle medium
FBS	Fetal Bovine Serum
HGMSCs	Human gingival derived mesenchymal stem cells
MSCs	Mesenchymal stem cells
NC	Neural Crest
OM	Osteogenic Medium
rhBMP-2	Recombinant human bone morphogenetic protein 2
SEM	Scanning Electronic Microscopy
VOI	Volume of interest

CHAPTER 1: INTRODUCTION

1.1 Background

Cleft palate is a congenital birth defect affecting soft and hard tissue of the craniofacial complex with an incidence of 1:700 births yearly [1, 2] (Figure 1.1). The incidence correlates with geographic origin, ethnic background, and socio-economic status. Palatal fusion is normally completed in man as bilateral palatal shelves grow and fuse to complete the palate formation at week 12. However, clefting of the palate is formed when there is a disturbance in palatogenesis process [1]. There are many variations of cleft palate and significant morbidities associated with this disorder resulting in a Health Burden [3].

Cleft lip and palate patients present with an extensive lists of challenges. Due to the anatomical imbalances and abnormal craniofacial growth and development, patients present with complications such as feeding problems, middle ear infection, speech abnormality, poor dentition, and psychosocial development. A craniofacial team is required to rehabilitate these patients providing a multidisciplinary approach with surgical and non-surgical life long therapies [4].

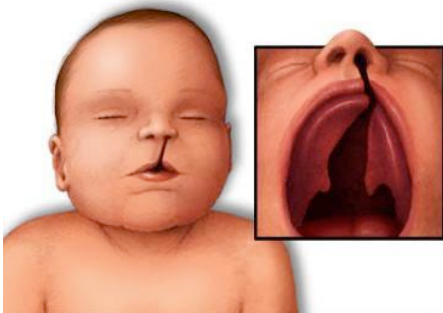


Figure 1.1: Cleft palate photograph. Extra oral and intraoral photograph of patient with unilateral cleft lip and palate.

1.2 Current surgical procedures

The available surgical procedures for the repair of cleft palate require a series of procedures throughout the course of a child's life to guide their craniofacial development (Table 1.2). The abnormality of children with cleft lip and palate requires such extensive intervention consisting of multiple surgical approaches in order to establish proper maxillofacial growth [2].

Current Surgical Procedures		
Age	Surgical Procedure	References
3-6 months	Definitive cleft lip repair to allow normal growth of nasiolabial complex	Behnia et al, 2009
10-14 months	Gingivoperiosteoplasty, closure of nasal mucosa and mucosa of the hard and soft palate to close oral-nasal communication; aiding infant in feeding, speech development, growth	Meng et al, 2009
5-10 years	Bone graft is performed to close hard tissue providing arch stability for the developing dentition	Meng, 2009 Greenwald 2001
13-18 years	Orthognathic surgery for maxilla bone advancement as needed to provide proper jaw relationship	Meng 2009 Conjero 2006
13-18 years	Rhinoplasty is performed to provide cosmetic corrections to the midface	Witt, Hardest, et al, 1993

Table 1.2: Current surgical procedures

Early in the child's life, soft tissue procedures offer limited repair leaving severe abnormalities in the maxillofacial growth requiring hard tissue repair. Therefore, the main procedure of cleft palate repairs the bone graft to provide closure of hard tissue. The objectives of hard tissue closure is to provide support for unerupted teeth and teeth

adjacent to the cleft, provide support for the lip and nose to improve symmetry, form stable continuous maxillary alveolar ridge, closure of oro-nasal fistula, support elevation of the alar base, and stabilization of the pre-maxilla in bilateral cases [1, 5-7]. In current clinical practice of cleft repair in humans, autologous bone grafts are utilized during the hard tissue surgery [2].

1.3 Complications

Autologous grafts are considered the “gold standard,” however requiring huge amount of bone [2, 4, 6, 8, 9]. Therefore autografts have limited availability and the harvest is often associated with donor-site morbidity [4], with the consequent drawbacks in terms of costs, procedure time, and patient discomfort [6, 10]. After repair, children still face abnormal maxillofacial growth resulting in midface deficiency requiring maxilla expansion and orthognathic surgery to improve facial appearance and dental function. Due to these limitations and disadvantages, alternative therapeutic methods are warranted to provide better treatment for children. On the other hand, allografts, the alternative to autografts, are being used in clinical practice over the last three decades [6, 11, 12]. However, allografts may carry with it the risk of disease transmission results in slow rate of new bone formation, may elicit immune response [13]

1.4 Paradigm shift

Tissue engineering techniques as alternative to traditional methods have emerged recently offering novel approaches to produce bone graft substitutes.

1.5 Tissue engineering

Tissue engineering/regenerative medicine strategies involves replacement of damaged or diseased tissue to maintain or improve tissue function applying biological and engineering principles [14, 15]. Essentially cell based tissue regeneration mimics natural

way of tissue regeneration. The cell based tissue engineering triad consists of stem cells, extracellular matrices (scaffolds), and pertinent biologic signaling molecules (Figure 1.5) [14, 16].

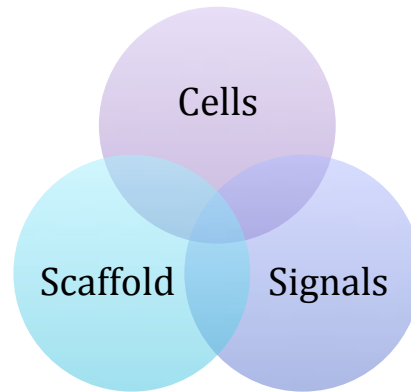


Figure 1.5: Tissue engineering concept. Tissue engineering is the summation of three components; scaffolds, cells, and signals.

1.6 Cells

Mesenchymal stem cells (MSCs) have emerged as potential cell sources in all cell based therapies [8, 17-20]. MSCs are adult stem cells that have ability to differentiate into a variety of cell types including osteoblasts, chondrocytes, and adipocytes. MSCs have a great capacity for self-renewal while maintaining their multipotency [19-21].

1.7 Signals

Signals and growth factors can stimulate cellular growth, proliferation, healing, and cellular differentiation. In regards to tissue engineering, to provide optimal growth and repair, scaffold systems can be supplemented with growth factors such as bone morphogenetic protein 2, vascular endothelial growth factor, fibroblast growth factor, transforming growth factor, insulin-like growth factor, and etc. [22, 23].

1.8 Scaffolds

A scaffold is a 3D construct that serves as temporary support for the cells that needs to be delivered on to the defect site. Ideal scaffold should have intrinsic cell adhesion and

interaction, porosity to promote cell proliferation and differentiation and exchange of nutrients and metabolites, degradation properties such as ability to degrade at the rate that tissue is formed, mechanical stability to withstand stress bearing mechanical loads, adaptability to irregularities, responsiveness to growth and development changes and micro surgically implantable [14, 24-28].

1.9 Bone tissue engineering:

Traditionally, autologous bone graft is used for bone repair however due to aforementioned concerns, tissue-engineering approaches have aroused as cutting-edge technology for bone regeneration. Bone tissue engineering is an approach utilizing osteogenic cells, osteoinductive signals, and osteoconductive scaffolds. Nevertheless, bone repair strategies in adults cannot be applied to the pediatric population as their bones are still in the developmental stages [14, 16]. Additionally, special considerations must be taken into account as cranial structures develop differently from appendicular skeleton and that the cranial structures are derived from neural crest derived MSCs [16]. This creates a unique challenge to develop tissue-engineering systems with the ability to recapitulate the corresponding craniofacial developmental events and needs. Therefore it is essential to select appropriate cell source and scaffold material. In this study, HGMSCs have been used as source of cells.

1.10 Human Gingiva Derived Stem Cells:

Bone marrow stem cells (BMSCs) are traditional stem cell sources [12, 16, 21, 29] for bone tissue engineering with the advantages of being an autologous source. However, there are several disadvantages as isolation involves invasive procedures. Furthermore BMSCs provide low yield of MSC with high variability and limited self-renewal capacity

(Figure 1.10) [17, 30]. The other sources of MSCs are from adipose tissue [4], human umbilical cord [30], human exfoliated deciduous teeth [31], and human dental pulp [32].

Recently, the human oral mucosa and gingiva has been discovered to be a promising alternative cell source for MSCs based tissue engineering [33]. HGMSCs derived from gingiva have been shown to be superior than bone marrow derived mesenchymal stem cells (BMMSC). HGMSCs have been shown to be easier to isolate, uniformly homogenous, proliferates faster than BMMSC, displays stability in long-term cultures, is not tumorigenic, and is independent of growth factors for expansion [17]. Recent evidence showed that HGMSCs are capable of immunomodulatory functions and anti-inflammatory function [20]. These reports suggest that gingiva derived stem cells may reduce healing time, scar tissue formation, and fistula formation [34].

HGMSCs have also recently been considered as an appropriate stem cell source for the repair and regeneration of bone in all craniofacial defects. 90% of HGMSCs are derived from cranial neural crest cells (CNCC) and 10% from the mesenchyme [19, 20, 35]. Neural crest cells are multipotent migratory cells unique to vertebrates that give rise to a diverse cell lineage such as melanocytes, neurons, tooth structure, and craniofacial cartilage and bone. Notably, post migratory CNCCs preserve stem cells reveal it's ability to regenerate craniofacial structures [19, 36]. Keeping in mind the several advantages of HGMSCs, this study intended to investigate the bone regeneration/formation capacity of HGMSCs.

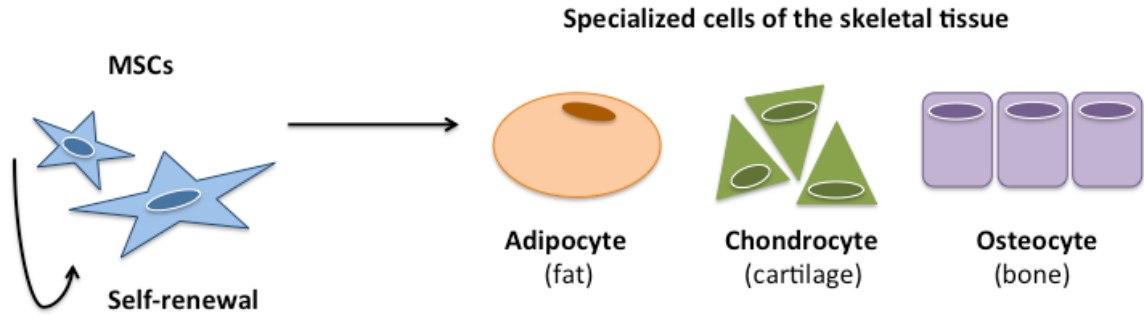


Figure 1.10: Mesenchymal Stem Cells. MSCs retain ability to self-renew and differentiate.

1.11 Injectable hydrogels

Traditional bone grafting techniques have complications of a large surgical scar, increased pain, and extended healing time. Hydrogels scaffold materials are attractive sources as they have structural similarity to the macromolecular-based components in the body and are biocompatible. Injectable hydrogels are novel strategy for local delivery of stem cells (Figure 1.11) [14, 24, 25]. Additionally these materials act as a dynamic liquid support to carry living cells, drugs and growth factors. They may be natural [14, 24] or synthetic [14, 24, 26] and have the ability to deliver cells at the defect site without inflammatory reaction with minimal immune response and reduce scar formation [24, 25].



Figure 1.11: Injectable peptide hydrogel scaffold. Scaffold with characteristic to deliver cells via injectable method.

1.12 PuraMatrix™

PuraMatrix™ is a commercially available self-assembled synthetic peptide hydrogel that is amphiphilic in nature. The peptide hydrogel is composed of 16 peptides with a repeating sequence of arginine, alanine, aspartate, and alanine (RADARADARADARADA or RAD16) (Figure 1.12A). The amino acid sequence consists of alternating hydrophobic and hydrophilic side groups (13, 14, 19). Most notably PuraMatrix™, upon contact with physiological conditions can instantly polymerize forming matrices providing three-dimensional architecture to the cells [27, 34, 37-41] (Figure 1.12B). The nanofiber structures of these peptides (<10nm in diameter with several times thinner than the cells) and the porous structure (5-200nm) enable the cells to grow within the gel. Furthermore, these fibers surround the cells in a manner similar to the natural extracellular matrix [42, 43]. Unlike the other extracellular matrix proteins such as collagen, laminin, and polyglycosamine materials, it is not animal derived. Previous studies have demonstrated that PuraMatrix™ can support cell attachment, proliferation, and differentiation in to various cell types [26, 44-47]. Also, the viscosity of the hydrogels allows injectable applications to fill irregular shapes and voids as presented by cleft palate defects to maximize cell adhesion and interaction enhancing bone regeneration [37]. This suggests that the PuraMatrix™ scaffold system is favorable to deliver the human gingival stem cells for the repair of bony defects including cleft palate.

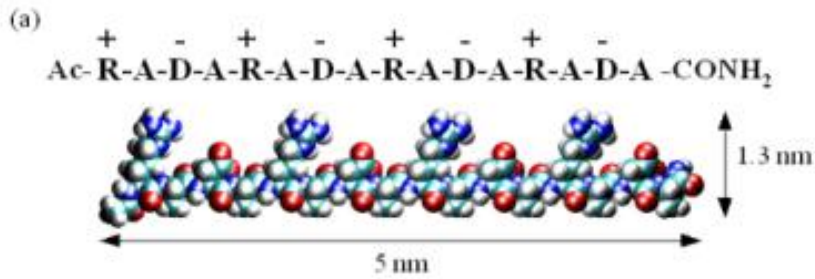


Figure 1.12A: PuraMatrix™ structure. RAD16 amino acid make up.

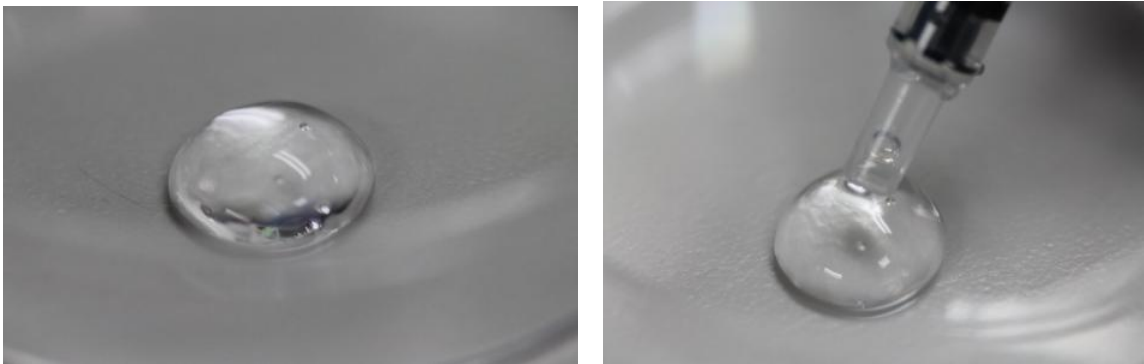


Figure 1.12B: PuraMatrix™ gel.

1.13 Objective

The objective of this study is to evaluate bone formation ability of a novel nano composite cell-scaffold system. Self-assembled nanofibrous peptide scaffolds in combination with HGMSCs were used for this study. Upon successful establishment, this scaffold system will be used to repair the hard palate.

1.14 Specific Aims and Hypothesis

1.14.1 Specific Aim 1: Characterizing cell-gel constructs of HGMSCs and PuraMatrix™

The first specific aim of this study was to evaluate cellular characteristics of HGMSCs encapsulated in the peptide hydrogel scaffold, PuraMatrix™, compared to cells cultured in

monolayer. Utilizing *in vitro* studies; cell proliferation, cell viability, confirmation of MSCs properties, and osteogenesis differentiation will be observed.

1.14.2 Specific Aim 2: Evaluate Bone formation capacity of HGMSCS embedded in PuraMatrix™ hydrogel

The cells were transplanted on to the subcutaneous sites of rats by either injected or implanted. In Injectable method, HGMSCs were cultured using standard culture conditions and induced with osteogenic differentiation medium for 9 days loaded onto PuraMatrix™ gel and injected in subcutaneous pockets of rats. In implantation method, HGMSCs were encapsulated and cultured in PuraMatrix™ hydrogel (3-D cultures) for 9 days and implanted in subcutaneous pockets of rats. The bone formation was monitored at 2 weeks and 4 weeks interval.

1.14.3 Hypothesis

Null Hypothesis (H_0): There is no difference in ectopic bone formation via subcutaneous implantation between HGMSCs seeded PuraMatrix™ scaffold compared to PuraMatrix™ scaffold only when measured by CT scans and histological analysis at 4 weeks.

Alternative Hypothesis 2 (H_1): There is significantly more ectopic bone formation via subcutaneous implantation of HGMSCs seeded PuraMatrix™ scaffold compared to PuraMatrix™ scaffold only when measured by CT scans and histological analysis at 4 weeks.

1.15 Location of study

This study was conducted at the Craniofacial Research Center (Room #7391), College of Dental Medicine, 3200 South University Drive, NOVA Southeastern University, Fort Lauderdale, FL 33328.

CHAPTER 2: MATERIAL AND METHODS

2.1 Overall study design

The study design consisted of two phases. The first phase was to isolate HGMSCs and to encapsulate HGMSCs in PuramatrixTM scaffold and monitor the cell growth and osteogenic potential. The second phase of the study investigates the *in vivo* efficacy of bone formation of HGMSCs in combination with the self-assembled scaffold.

2.1.1 Specific Aim 1: Characterization of PuraMatrixTM Scaffold impregnated with HGMSCs

Healthy discarded human gingival tissue was obtained with the informed consent from the patients undergoing the flap surgeries and crown lengthening procedures at NSU Dental Clinics. Mesenchymal stem cells were isolated from the gingival tissue (NSU IRB #02071304) and expanded under standard culture conditions. The panel of surface makers (CD73⁺, CD90⁺, CD105⁺ and CD34^{-ve}) was measured on regular basis (to each batch of the MSCs) to confirm their stem cell nature. Our pilot studies have shown that the cells encapsulated in 0.5% PuramatrixTM have enhanced proliferation over 1% PuraMatrix scaffold. Therefore, we propose to use 0.5% PuraMatrix for this study. We investigated cell proliferation and differentiation of HGMSCs within the hydrogel scaffold (Figure 2.1.1).

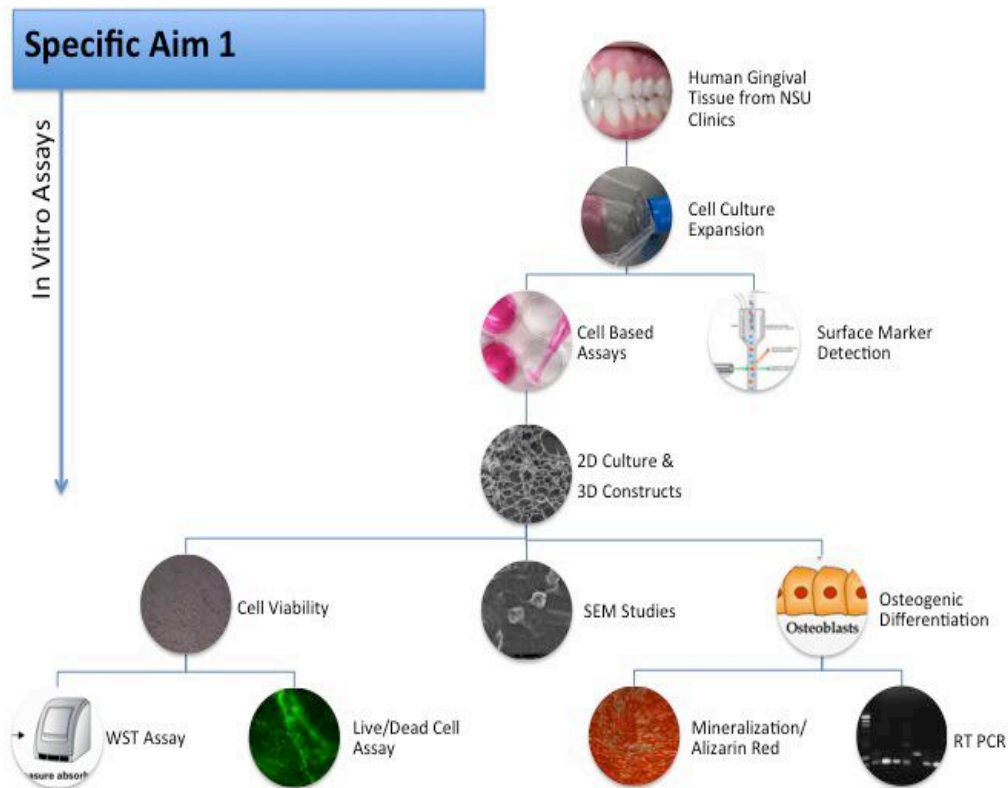


Figure 2.1.1: Specific Aim flow chart

2.1.2 Specific Aim 2: *In vivo* evaluation of bone formation ability of composite injectable cell- scaffold system

Two types of cell delivery methods were evaluated for bone formation ectopic bone formation model. **Method 1.** Cells in monolayers (2-D cultures) were cultured and guided for osteogenic differentiation for 9 days. On Day 10 the cells were mixed with Puramatrix™ and injected using a syringe with 20 gauge needles in subcutaneous sites

Method 2. The cells encapsulated in 0.5% Puramatrix™, cultured and differentiated (3-D cultures), and delivered in subcutaneous sites. Detailed experimental procedures were given below. The bone formation was followed at 2 and 4 week time intervals. Bone growth was assessed with computed tomography (CT) scan and histologically. The

results of this subcutaneous model study determined the more suitable implantation and delivery mode of cell-scaffold system (Figure 2.1.2).

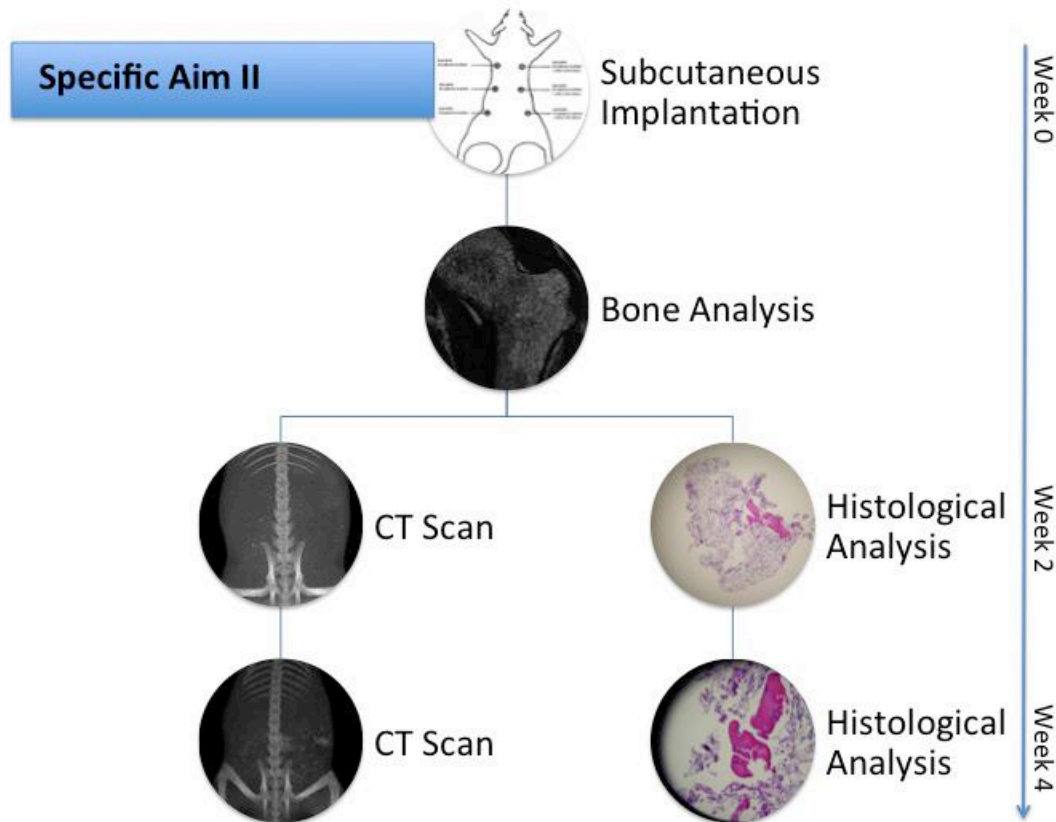


Figure 2.1.2: Specific Aim 2 flow chart

2.2 Materials

Commercially available self-assembled peptide scaffold PuraMatrix™ obtained from Corning Life Sciences (Tewksbury, MA) was used for the study. HGMSCs were obtained from human gingival tissue from clinic at Nova Southeastern University (Davie, FL) upon the approval of institutional review board. For the use of Sprague Dawley rats, Institutional ethical clearance was obtained (# 053-468-0121) prior to the commencement

of the study. Unless otherwise mentioned, all other necessary chemicals and lab supplies required for the study were obtained from Sigma (St. Louis, MS), from VWR international (Radnor, PA) respectively.

2.3 Isolation of mesenchymal stem cells from gingival tissue

The gingival tissue obtained from clinic was de-epithelialized and minced into small pieces (2x2mm) and rinsed with Dulbecco's Modified Eagle Medium (DMEM; Life technology, Carlsbad, CA) supplemented with 10% fetal bovine serum (FBS; Atlanta Biologics, Norcross, GA), 400 mmol/ml L-glutamine, 100 U/ml penicillin, 100 lg/ml streptomycin and 1% amphotericine [48]. Mesenchymal stem cells were obtained from the gingival tissue using standard procedures [17]. Briefly, cells were digested enzymatically using collagenase and dispase for 30 minutes. The first cell suspension was discarded to avoid the interference of epithelial cells. The tissue samples were further treated with collagenase and dispase and the cell suspension was collected. The procedure was repeated twice and the cell suspensions were pooled. The cell suspensions were centrifuged and the cell pellet were plated in tissue culture flask and grown under standard culture conditions, in a humidified incubator at 37°C and 5% CO₂.

2.4. Cell Culture

Cells cultured under specific culture conditions were subsequently sub-cultured at 90% confluence [5] and expanded. The cells were cultured in growth medium (DMEM, 10% FBS and 1% antibiotics) at 37°C and 5% CO₂. To ensure uniform cell population first two passage cells were kept further expansion and cells from third or fourth passage were used for all studies.

2.5 Characterization of HGMSCs by surface markers by flow cytometry method

Cells at the concentration of 10^6 cells were used to measure the surface markers using Miltenyi Kit according to manufacturer's instruction. The specific markers positive for mesenchymal stem CD 73, CD 90 and CD 105 and negative for CD 34 were identified at the facilities at University of Miami using a florescent activated cell sorter FACSAria IIIu (BD Biosciences, San Jose, CA) with adjusted florescence compensation setting negative samples were used to set up the thresholds of quadrant markers (Figure 2.5).

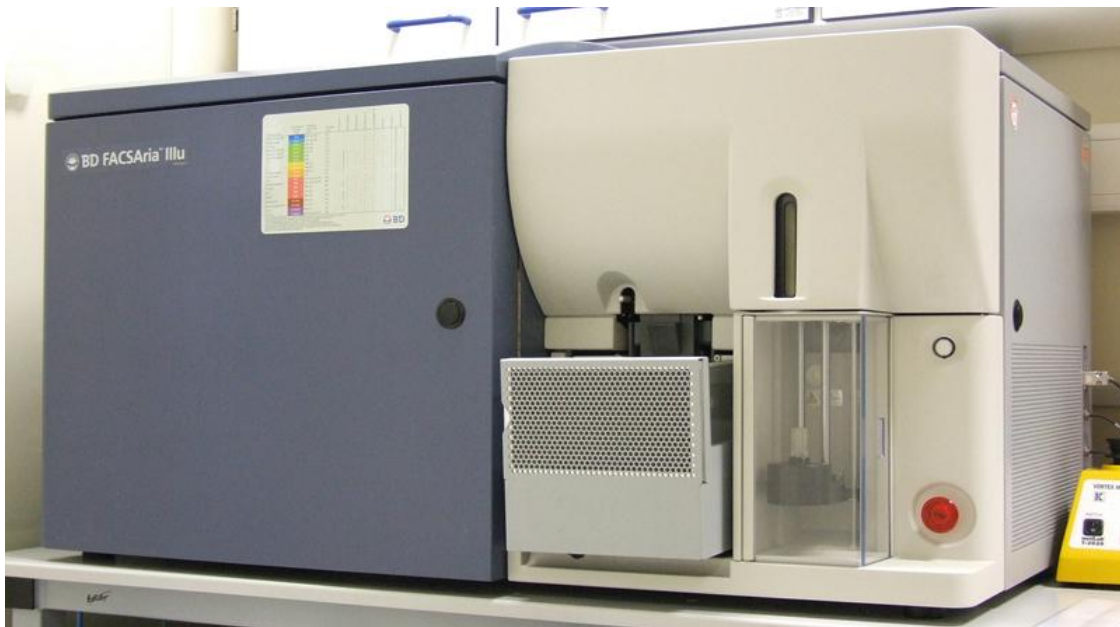


Figure 2.5: Flow cytometry. BD FACSAria IIIu

2.6 HGMSCs encapsulation and culture in Puramatrix™ (cell-gel Constructs 3D culture) scaffold:

The cells (HGMSCs) from 3rd or 4th passage were used for all of experiments. Based on our pilot studies and previous literature [49] support we have chosen to use 0.5% Puramatrix™ for all the experiments. The encapsulation method was followed according to manufacturer's instructions. Briefly, the cells were suspended in 20% filter sterile

sucrose solution (isotonic) and combined at 1:1 with 1% Puramatrix™. To form cell-hydrogel complex, 500 µL of standard culture medium was added to each well of a 24-well tissue culture plate, and cell- gel mix was slowly dropped in to each well of 24 well plate. To prevent drying of the surface of hydrogel, the culture medium was carefully layered and incubated in 37°C at 5% CO₂ for 30 min. The medium was replaced after designated time to equilibrate the physiological pH conditions. The cell-gel constructs were further incubated under standard culture conditions and cell morphology was monitored under phase contrast microscope on daily basis. The growth pattern was carefully monitored to check whether encapsulation of HGMSCs in the peptide hydrogel scaffold is damaging.

2.7 Scanning Electronic Microscopy studies

The cells were encapsulated in 0.5% Puramatrix™. Puramatrix™ hydrogel alone and the cell gel constructs at day 3 and Day 7 were used for the study. The cell-gel constructs were washed with PBS and were fixed in 2% gluraldehyde solution and dehydrated in graded series of alcohol and snap fractured and critical point dried from CO₂. Samples were mounted and gold sputtered and examined under SEM (Quanta 200; FEI, Hillsboro, OR, USA) (Figure 2.7).



Figure 2.7: Scanning Electron Microscope: FEI Quanta 200

2.8 Cell Viability

2.8.1 WST assay

Cell proliferation was assessed by addition of WST-1 (2,4-dinitrophenyl)-5-(2,4-disulfophenyl)-2H-tetrazolium, monosodium salt) reagent to a 1:10 final concentration. WST-1 cell proliferation assay (Roche, Indianapolis, IN, USA) is a mitochondrial activity assay. WST reagent is a soluble tetrazolium salt that can react with metabolically active cells and gives a deep red color. 96 well plates were used for this assay, in order to prepare for cell-gel constructs 200 μ l of growth medium was placed in each well of the plate. Cells suspended in 0.5% gel were slowly released into the growth medium. After 30 minutes of the incubation at 37°C the growth medium was replaced and cells were fed with new growth medium and gelation was examined under microscope. The cell-gel constructs were finally incubated at 37°C, 5% CO₂. The assay

was conducted at 24, 48 and 72 hours' time intervals and the absorbance was measured using micro-plate reader (Figure 2.8.1). The cell viability was expressed in percentages.

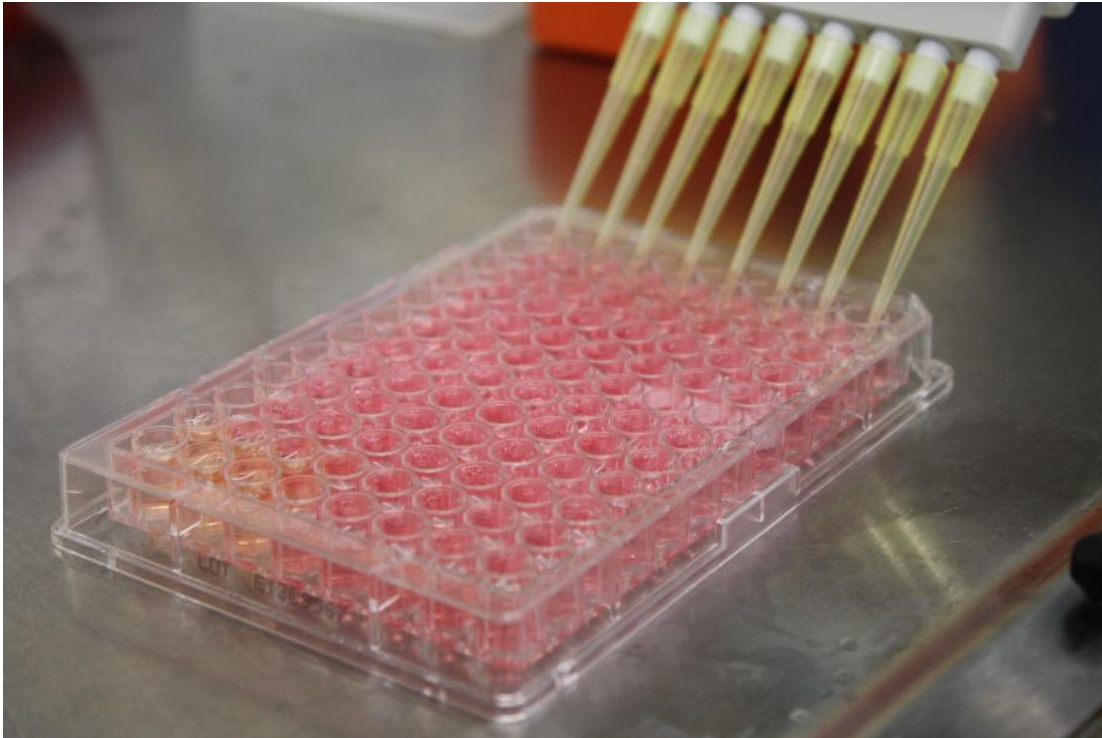


Figure 2.8.1. WST Assay.

2.8.2 Live Dead Cell Assay

Cell viability of the HGMSCs in PuraMatrix was assessed by another assay called Live/Dead cell assay (Molecular Probes, Carlsbad, CA) (Figure 2.8.2). Cells were grown in PuraMatrix and cell proliferation was followed at 1, 3, 5, and 7 day intervals. Live Dead cell assay kit provides two molecular probes, calcein AM and ethidium homodimer-1 (Eth-D) for simultaneous visualization of the live cells and dead cells. Live Cells emit Green Fluorescence when calcein AM enters the cells and is hydrolyzed to calcein by intracellular esterase. Eth_D 1 enters to nucleic acids to produce bright red fluorescence.

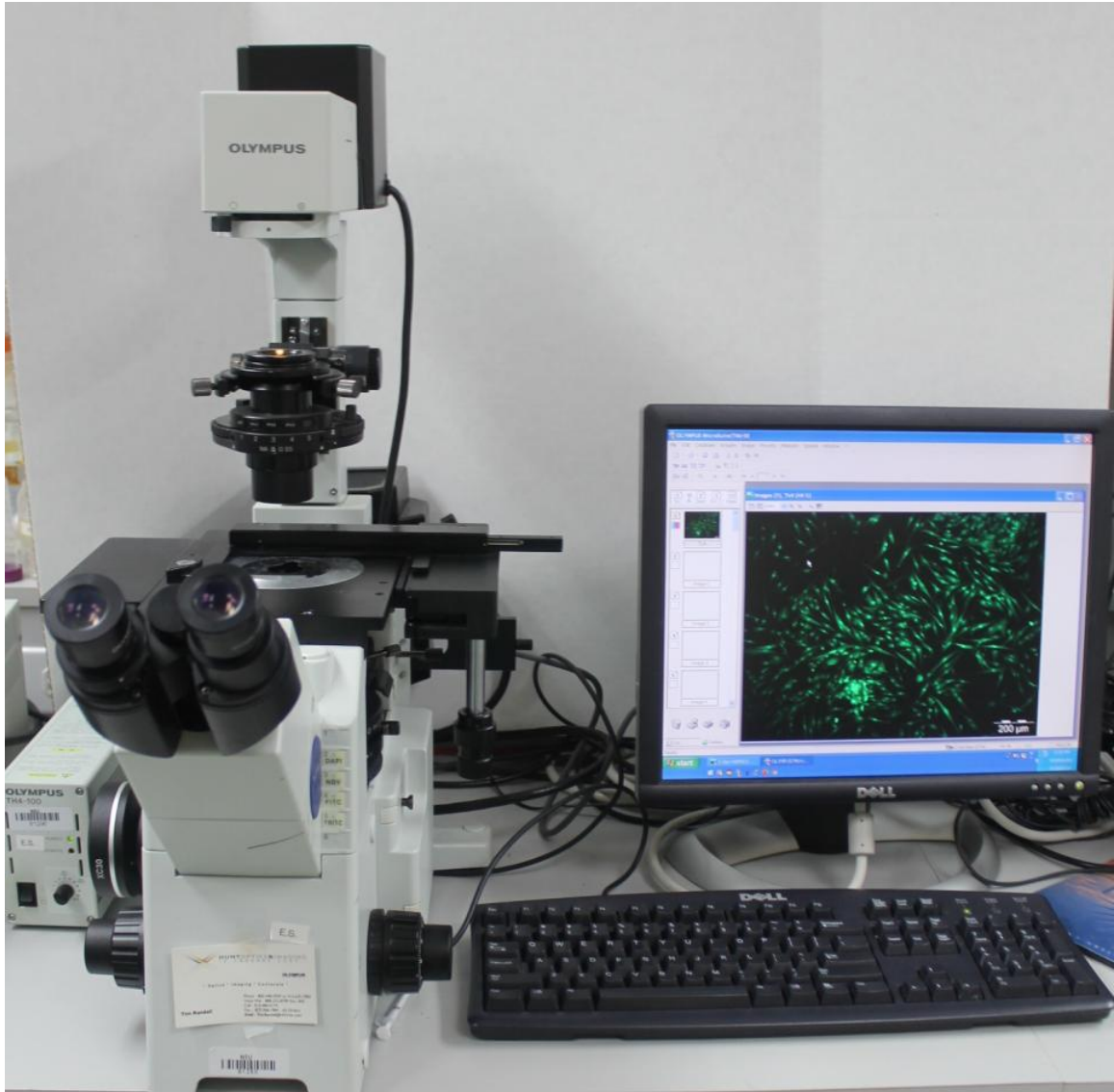


Figure 2.8.2: Live/Dead Cell Assay: Olympus IX51

2.9 *In vitro* confirmation of osteogenic differentiation

PuraMatrix™ in combination with stem cells can induce osteogenic differentiation in the presence of osteogenic supplements [27]. We have monitored the osteogenic differentiation of cells in the constructs at weekly intervals. For the differentiation assays 24- well plates were used. The cells suspended in 20% of sterile sucrose (250 μ L) with 250 μ L of 1% PuraMatrix™ and dropped slowly in to growth medium in which the

scaffold can self-assemble to acquire gel shape. The gelation was observed under microscope. The gene expression of osteogenic markers was investigated using RT PCR and matrix mineralization was monitored at 1, 2 and 3 weekly intervals.

2.9.1 Gene expression assay (RT PCR)

The cell-gel constructs were induced with osteogenic supplements after 5 days of culture period. The constructs with only growth medium were considered as control. The constructs incubated for 2 weeks was assessed for gene expression studies. Briefly, the cells were released from the gel by mechanical disruption and RNA was extracted using Trizol (Life Technologies, Carlsbad, CA) method according to manufacturer's instruction. RNA was quantified and cDNA was measured using to standard protocols. Semi-Quantitative PCR was conducted using specific primers (Table 2.8.1) and the PCR products were separated by 2% agarose gel and the relative density was measured using a densitometry analysis.

Gene	Sequence
Col I (sense)	5'-ctgaccttctctgcgctgatgtcc-3'
Col I (antisense)	5'-gtctggggcaccaacgtccaaggg-3'
ALP (sense)	5'-ccacgtcttcacatttggtg-3'
ALP (antisense)	5'-agactgcgctgtagttgt-3'
OPN (sense)	5'-tgaacgagtcagctggatg-3'
OPN (antisense)	5'-tgaattcatggctgtggaa-3'
beta-actin (sense)	5'-catgtacgttgctatccaggc-3'
beta-actin (antisense)	5'-ctccttaatgtcacgcacgat-3'

Table 2.9.1 Specific primers

2.9.2 Matrix mineralization using Alizarin Red Stain

The monolayer cells and cells encapsulated in PuraMatrix™ were investigated and compared for their osteogenic potential. Matrix mineralization was monitored sequentially on weekly basis. The calcium deposition was confirmed by staining the cells with Alizarin red S staining protocol. Briefly, cell in monolayer or constructs cultured in osteogenic medium for 4 weeks were fixed with 10% formalin for 30 minutes at room temperature and then washed with phosphate-buffered saline for 5 minutes followed by 10 minutes of incubation with 1% alizarin red solution (Poly Scientific Corp., Bay Shore, N.Y.) incubated for 10 minutes at room temperature. Slides were then washed with running tap water for 5 minutes and left to dry. The same procedure were performed for undifferentiated mesenchymal stem cells [5].

2.10 *In vivo* study methodology

2.10.1 Animal subjects

For this study, 4-5 week Sprawley Dawley male rats were chosen (2.10.1). They were kept in animal holding facility in separate cages receiving adequate water and food pellets under automatically controlled temperature and lighting. Animals were allowed to acclimate to environment for 1-3 days. Pre-operative weight and length were measured. All intervention and care followed International Animal Care and Use Committee's approved protocol.



Figure 2.10.1: Sprague Dawley rat. 4-week old male

2.10.2 Anesthesia

Intramuscular injections of 1mg/kg intraperitoneal injection of 1:10 Xylazine: Ketamine solution was given prior to the surgery (Table 2.10.1) [50, 51] . Upon the onset of anesthesia, rat subjects were transported from animal facility to surgical lab. Repeated dosages of 0.5mg/kg were administered as needed per procedural protocol established in our research laboratory.

10ml 1:10 Xylazine: Ketamine anesthetic solution	
Xylazine 20mg/ml	2.5 ml
Ketamine 100mg/ml	3.75 ml
Sterile Water	3.75 ml

Table 2.10.1: Veterinary anesthetic concentration

2.10.3 Cell Culture and differentiation

Cells necessary for animal experiments were cultured and differentiated in two different methods. For injectable mode of transplantation monolayer cell cultures were guided to differentiate for 9 days and on day 10 the cells were used for injections. The cells used for implantation method were encapsulated in Puramatrix™ and induced with osteogenic supplements for 9 days and on 10th day the cell- gel constructs were implanted in the subcutaneous pouches at dorsum of the rat.

2.10.4 Subcutaneous implantation/ectopic bone formation

Total six rats (4-5week/200-250g) were used for this experiment. The rats were divided into three groups. 1. Control (without intervention) 2. Cells encapsulated in PuraMatrix™ and implanted subcutaneously (Preformed gel) 3. Cells grown in 2 D cultures were mixed with PuraMatrix™ instantaneously and injected (Injectable group). Intravenous injections of the immunosuppressant FTY720 (0.05mg/kg) were given to each rat [52] in order to prevent transplant rejection. The bone formation ability of each scaffold were analyzed *in vivo* using a subcutaneous pouch model described [53]. Briefly, six pouches were made by blunt dissection in subcutaneous sites [12]. The cells delivered either implantation mode or injectable mode.

Cell Delivery through implantation mode: Up to 0.5×10^6 cells were encapsulated in 0.5% PuraMatrix™ and the cell-scaffold mix were filled in the subcutaneous defect. The pouches were closed with silk sutures and monitored for recovery.

Cell Delivery by injectable mode: The cells cultured as monolayers (2D cultures) were osteogenically differentiated up to 9 days and on 10th day the cells were trypsinized and dislodged from the culture flask mixed with PuraMatrix™ gel and injected using a disposable syringe delivered through 20 G needle.

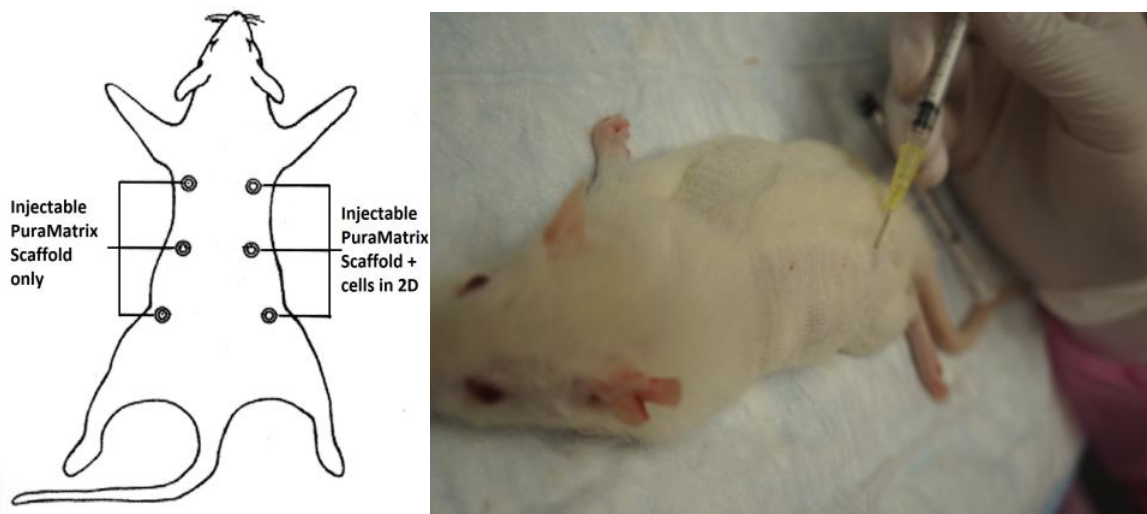


Figure 2.10.4A: Injectable group diagram and surgical photograph



Figure 2.10.4B: Preformed group diagram and surgical photograph

2.10.5 Post-operative care

Post-operative care was provided with buprenorphine for analgesia for 48 hours and with antibiotics, trimethoprim/sulfamethoxazole, for 10 days at 3mcg/kg [23]. A soft diet was prepared and provided for rats in the form of moist food pellets for 24-48 hours per animal care protocol established in our research laboratory. Rats were evaluated frequently for any signs of inflammation or necrosis [54]

2.11 Bone analysis

2.11.1 CT scans

CT scans were utilized to monitor bone formation and growth. Panoramic scans were taken for evaluation at 2 weeks and 4 weeks post-surgery. The relative bone areas were measured by CT scan using i-Cat vision software (Figure 2.10.1). The machine operates at 120 kVp and 22.85 mAs, acquiring 300 basis images in a single 20-second revolution around the rat head. High resolution scans produces images at 0.2 mm voxel size and 14 bit gray scale quality allows more shades of gray to increase contrast for easier viewing [55]. Each rat was sedated and placed on the same cephalostat and in a standardized manner with the head in natural position. Utilizing i-CAT software, 2D scans and 3D volumetric representation scans will be used to qualitatively identify and observe bone growth [54] . One-millimeter coronal sections of control and experimental findings will also be observed for quantitative measurements. Using Image-J software, total number of pixels of coronal sections was determined using manipulation color thresholds and selected for measurement. Radiopacities were then selected by free hand and measured. The extent of new bone area per total area was displayed as a percentage [4, 8, 12, 22].



Figure 2.11.1: CT scan

2.11.2 Histological analysis:

Following CT scans, animals were euthanized by CO₂ asphyxiation and explants were dissected at 4 weeks for histological analysis [51]. Samples were fixed in 10% neutral buffered formaldehyde for 24 hours and were sent to the Pathology Lab (University of Miami, Florida) for further processing. The protocols for microtome sectioning were followed using standard protocols. Briefly, after fixation the samples were processed using dehydration procedure and the samples were embedded in paraffin wax and 5 μ m sections were obtained from each sample and the sections were stained with Hematoxylin

and Eosin (H&E) staining and further histological analysis [37] was carried out. The injection of the mixture will be done by mixing PuraMatrixTM with the cells at a density of 2×10^6 cells/matrix and was injected in the defect [39]. The tissue samples were observed by an optical microscope (IX51; Olympus, Tokyo, Japan) and observed qualitatively for the appearance of new bone formation and quantitatively for relative surface area. Using Image-J software, total number of pixels of histological samples was determined using manipulation color thresholds and selected for measurement. Bone tissue were then selected by free hand and measured. The extent of new bone area per total area was displayed as a percentage [12, 56].

2.12 Statistical analysis:

To evaluate differences between or among groups, analysis of variance (ANOVA) will be performed. A P-value < 0.05 is selected for significance for the statistical tests.

CHAPTER 3: RESULTS

3.1 Isolation and culture of human gingival cells

Human gingiva derived stem cells were separated from the gingival tissue using enzymatic digestion technique as described in section 2.1. The cell suspension was seeded at a density of 2×10^4 cells/cm² and fed with growth medium (DMEM supplemented with 10% FBS and 1% antibiotics). The colony forming units were observed after 2 days of seeding. The cells reached 70 to 80% confluency after 7 to 8 days post seeding (Figure 3.1). The cell population was homogenous; cells were tightly adhered with spindle-shaped fibroblasts-like in appearance (Figure 3.1).

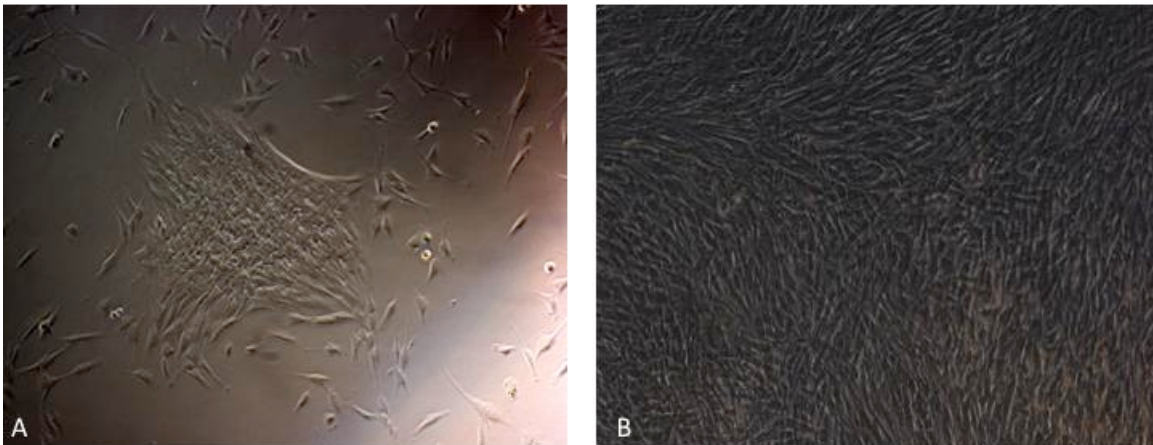


Figure 3.1. Isolated HGMSCs. A) Freshly isolated HGMSCs from tissue plated on T75 Tissue Culture Flask. B) Cells at confluence.

3.2 Flow cytometry analysis

The flow cytometry analysis is a screening assay to identify the panel of surface markers to identify MSCs. Cells at third passage were used for the flow cytometry analysis. The results confirmed positive for CD 73, CD 90, CD105 (all above 90%) and negative for hematopoietic stem cell marker CD 34 (Figure 3.2).

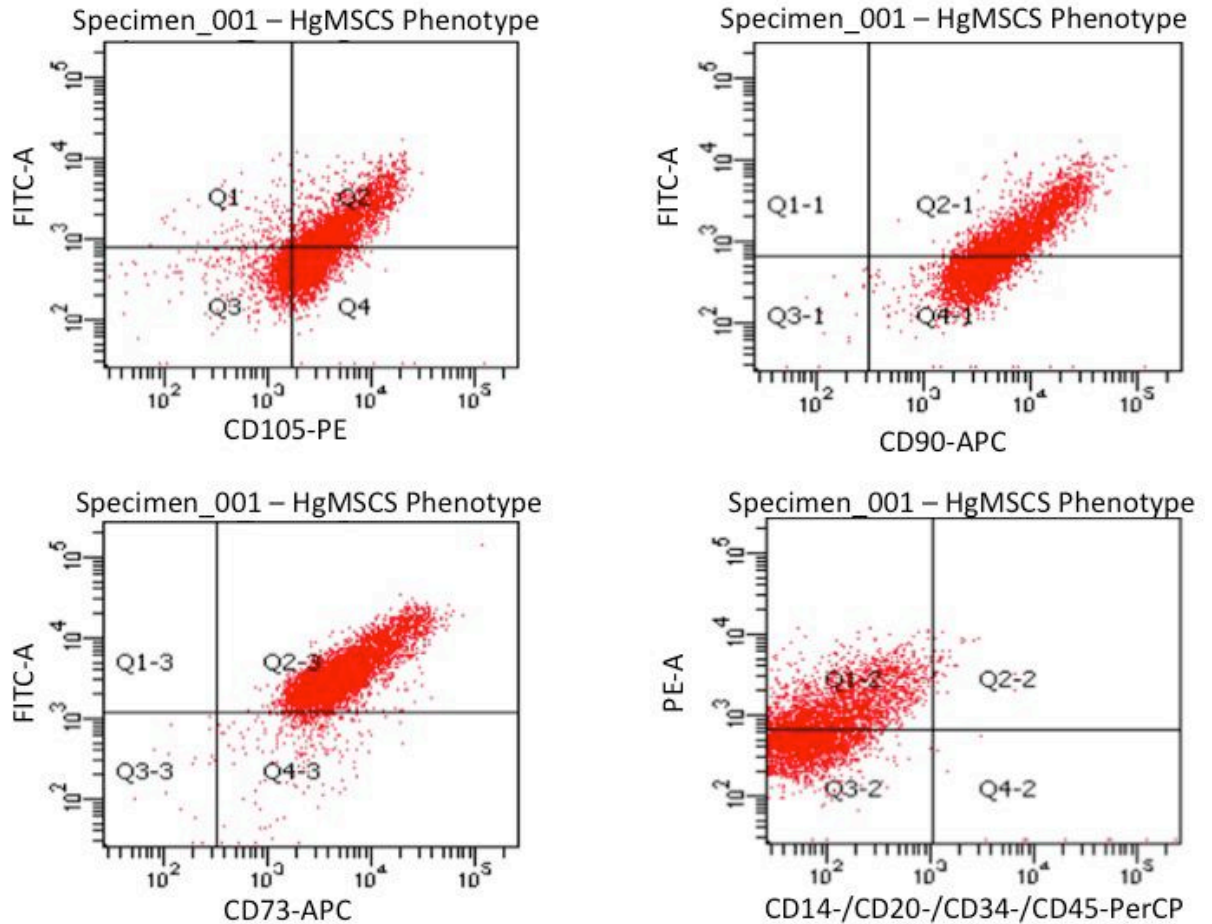


Figure 3.2. Flow cytometry analysis. Flow Cytometry shows that cells expressed markers characteristic of MSCs; positive for CD105, CD90, CD73, and negative for CD14, CD20, CD34, and CD45.

3.3 Cell Growth in PuraMatrix™ (cell –gel constructs 3D model)

For all our studies cells from passage 3 or 4 were used. The cells encapsulated in 0.5 % PuraMatrix™ as described in methodology section. Cell morphology and growth characteristics were monitored sequentially under light microscope.

3.3.1 Light microscopic observation

Under phase contrast view, HgMSCs seeded on to the PuraMatrix™ nano scaffolds showed spherical structures at Day 0. Cell growth was observed from day1. On Day 3

cells attained their original spindle shaped. The cells were integrated with in the gel, however the cells in the center appeared spherical. The cells in the center appeared cluster shaped and on peripheral region attained spindle shaped. On day 7 cells were well spread out. Following shows detailed morphological features (Figure 3.3.1 A-C).

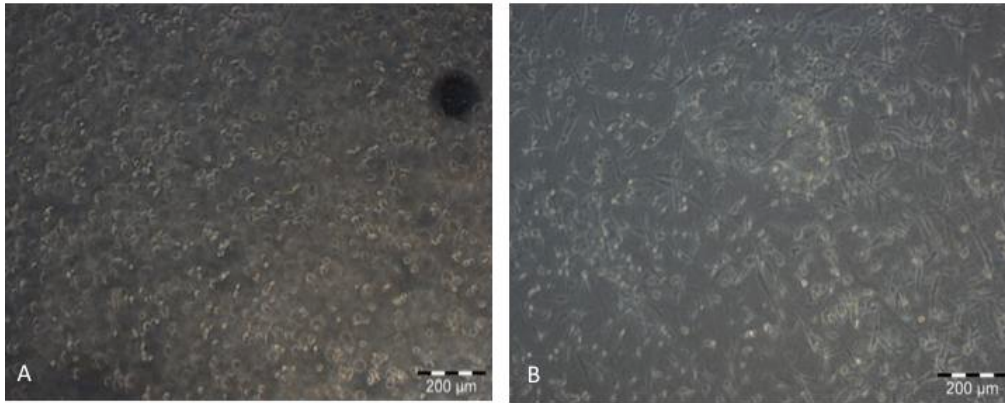


Figure 3.3.1A: Light microscopy of HGMSCs at Day 1 and 3. Cells encapsulated in PuraMatrix™ hydrogel; Phase contrast images showing the morphology and cell proliferation at different time points. A) Day 1- Cells show round structures. B) Day 3- Cells attained spindle shape- cell growth can be observed.

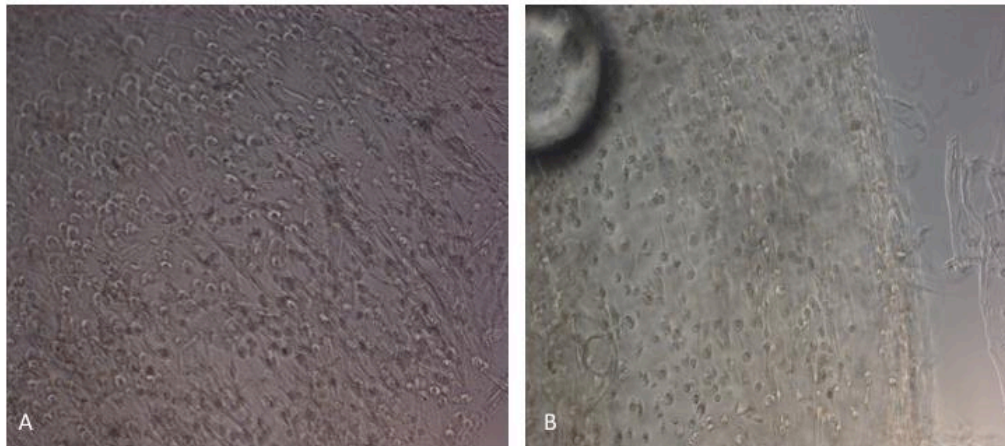


Figure 3.3.1B: Light microscopy of HGMSCs at day 5. A) Cells encapsulated in PuraMatrix™ B) Day 5- Cells at peripheral region

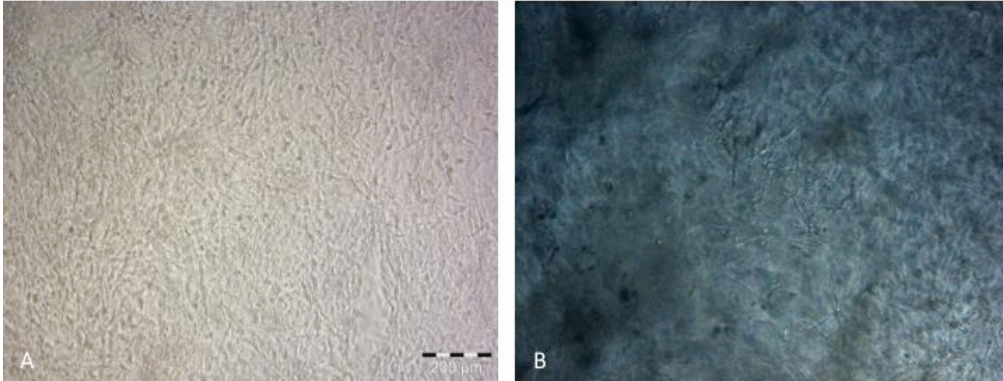


Figure 3.3.1C: Light microscopy of HGMSCs at day 7. A) Interconnection between the cells can be clearly seen B) Cells formed a network with in the nanofiber scaffold.

3.4 Scanning Electronic Microscopy studies

SEM studies demonstrated that the nanofibers are $\sim 10 - \sim 20$ nm. PuraMatrixTM scaffold without cells showed a sheath like structure in lower magnification. All observations made at cells at day 3 or day 7 cultures (Figure 3.4). The cell bodies appear to be fully embedded in the nanofiber scaffold. Cells at day 3 appeared clusters in the center and elongated in the peripheral region. However the cells were intimately interacted within the nanofiber. The cells at day 7 the cells showed a linear assembly with in the matrix.

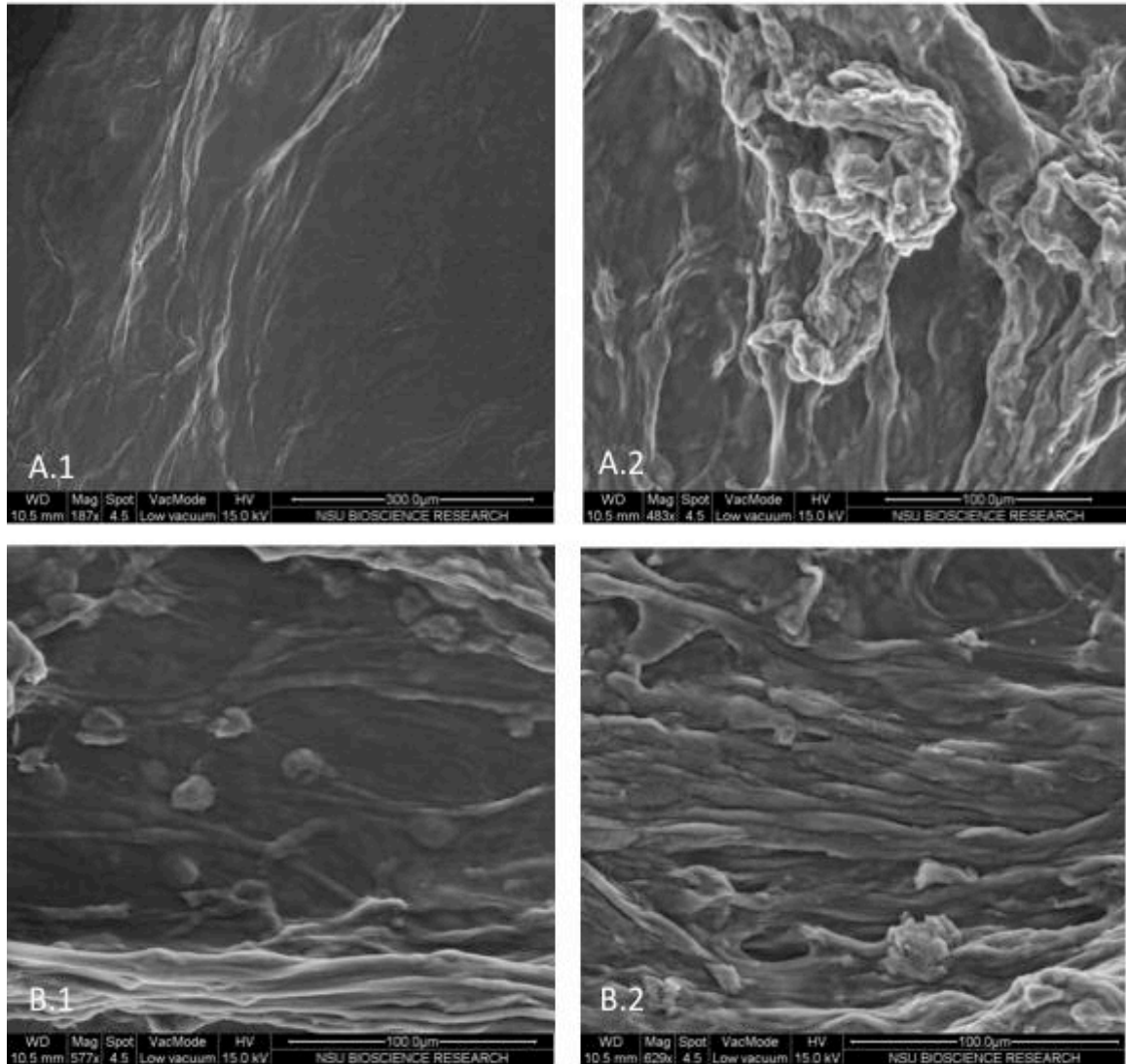


Figure 3.4: SEM of PuraMatrix™ and HGMSCs seeded PuraMatrix™. A) Scanning electron microscopy of PuraMatrix™ scaffold only. A.1 Shows surface appearing like a sheet under low magnification, 187x. A.2 Shows peptides appearance to be like interwoven nanofibers at higher magnification, 483x. B) Scanning electron microscopy of PuraMatrix™ with HGMSC cells. B.1 PuraMatrix™ with HGMSC under 577x magnification. Shows linear assembly of cells within matrix. B.2 PuraMatrix™ with HGMSC under 629x magnification. Shows linear assembly of cells within matrix

3.5 Cell growth in PuraMatrix™ (cell –gel constructs 3D model)

3.5.1 WST Assay

WST assay is a quantitative assay to measure the cell proliferation. The cell density at 1×10^4 was encapsulated in 0.5% PuraMatrix™ with and cell viability was observed at 1, 2 and 3 days of time interval. Our results revealed that there was slight increase in the percent viability within the group. However, there was significant increase in cell proliferation at the density of 300,000 on day 3 (Figure 3.5.1).

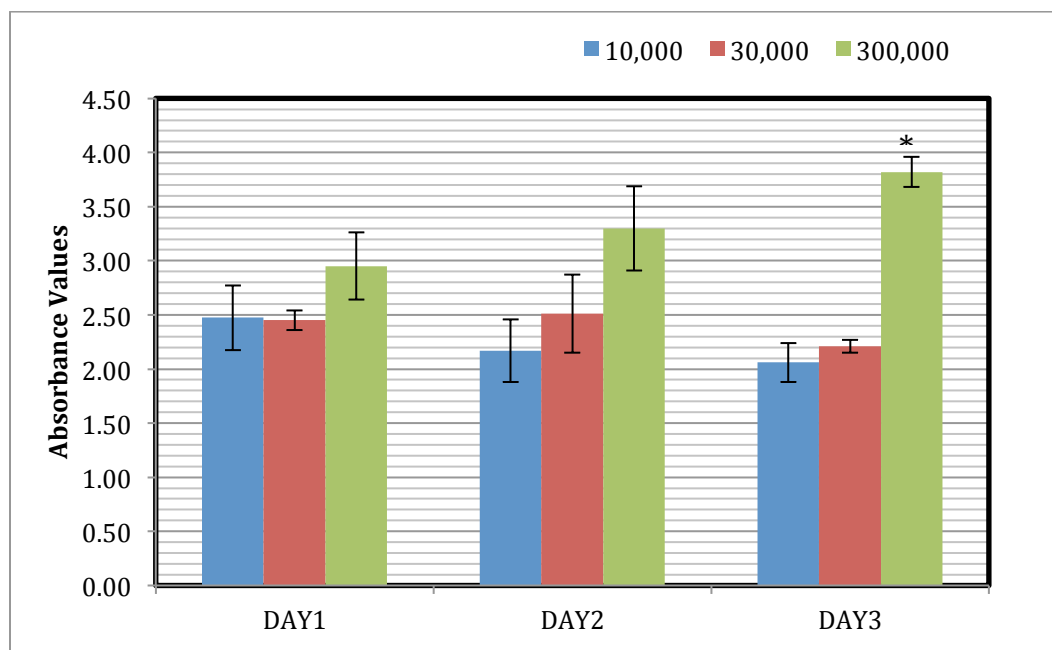


Figure 3.5.1: WST Assay graph

3.5.2 Live Dead Cell Assay

The cells were encapsulated and seeded on to a 96-well plate. For each gel 50μL of PuraMatrix™ was used to encapsulate the cells. The viable and dead cells were visualized using a fluorescence microscopy. The viability was investigated at different time points (1, 3, 5 and 7 days) indicated that cells were viable at all-time points observed. The cell growth started from day 1. At day 3, HGMSCs possessed spindle shape showing

typical MSCs feature. Although there was not significant cell proliferation there was an increase in number at day 3 (Figure 3.5.2).

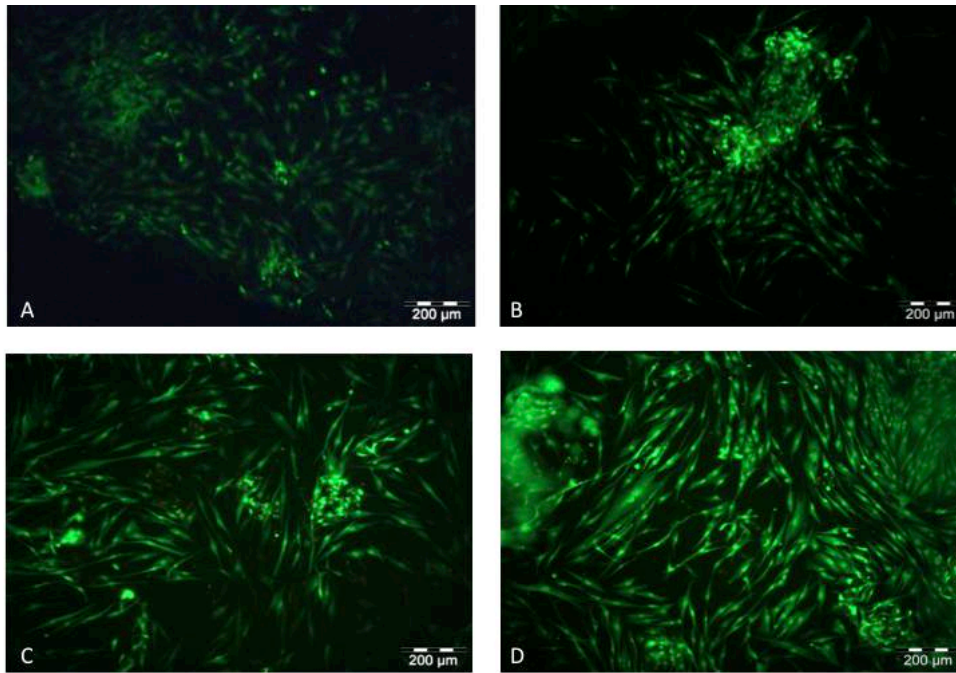


Figure 3.5.2: Live/Dead Cell Assay at day 1, 3, 5, and 7. Fluorescent microscope staining of cells in PuraMatrixTM hydrogel with Live/Dead staining. A) Day 1-Cells encapsulated on day one B) Day 3- Cells with spindle shape and they are spread out evenly. C) Day 5– Cells are alive and express growth. D) Day-7 Cells have increased in proliferation and show adhesion to fibrous network.

3.6 Osteogenic differentiation

3.6.1 Expression of osteogenic marker genes

Gene expression of osteogenic lineage specific genes was assessed by semi quantitative RT-PCR at 2 weeks' time interval. Cells encapsulated in PuramatrixTM induced with osteogenic medium showed up regulation of alkaline phosphatase and osteopontin and type I collagen gene expressions compared to control cell-gel constructs in culture medium (Figure 3.6.1).

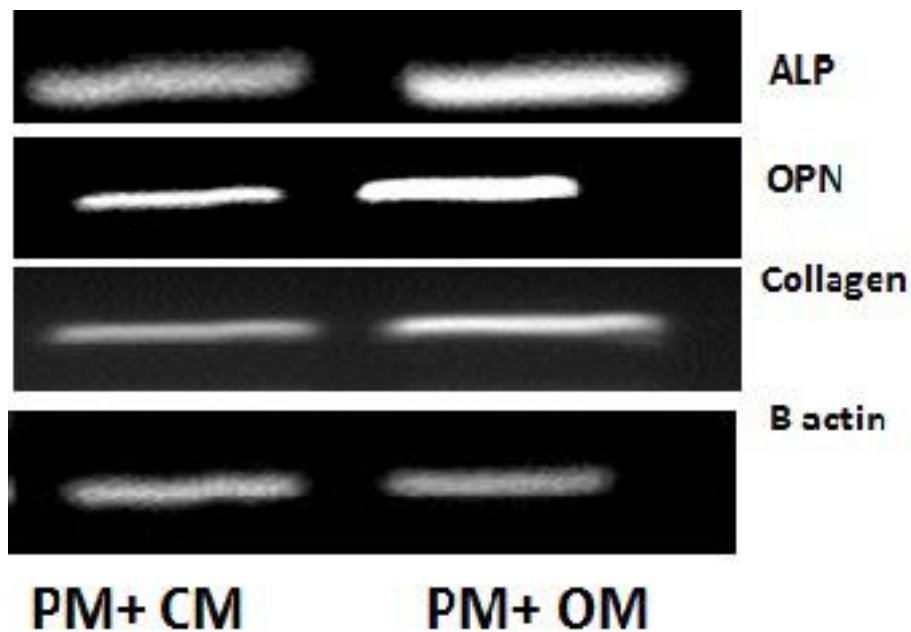


Figure 3.6.1: RT-PCR Assay

3.6.2 Matrix mineralization using Alizarin Red Stain

The cells induced with osteogenic differentiation medium were monitored at weekly intervals. Cells in the presence of osteogenic factors gingival cells showed formation of mineralized nodules or aggregates (Figure 3.6.2) at 4th week of the induction. Calcium mineralization was observed at week three after the induction of osteogenic medium. This was cells encapsulated in PuraMatrixTM was confirmed by Alizarin red S staining. Alizarin red is anthroquinone dye to stain the calcium deposits which are indicators of mature osteocytes [57]. The mineral deposition is detected by the orange color nodules.

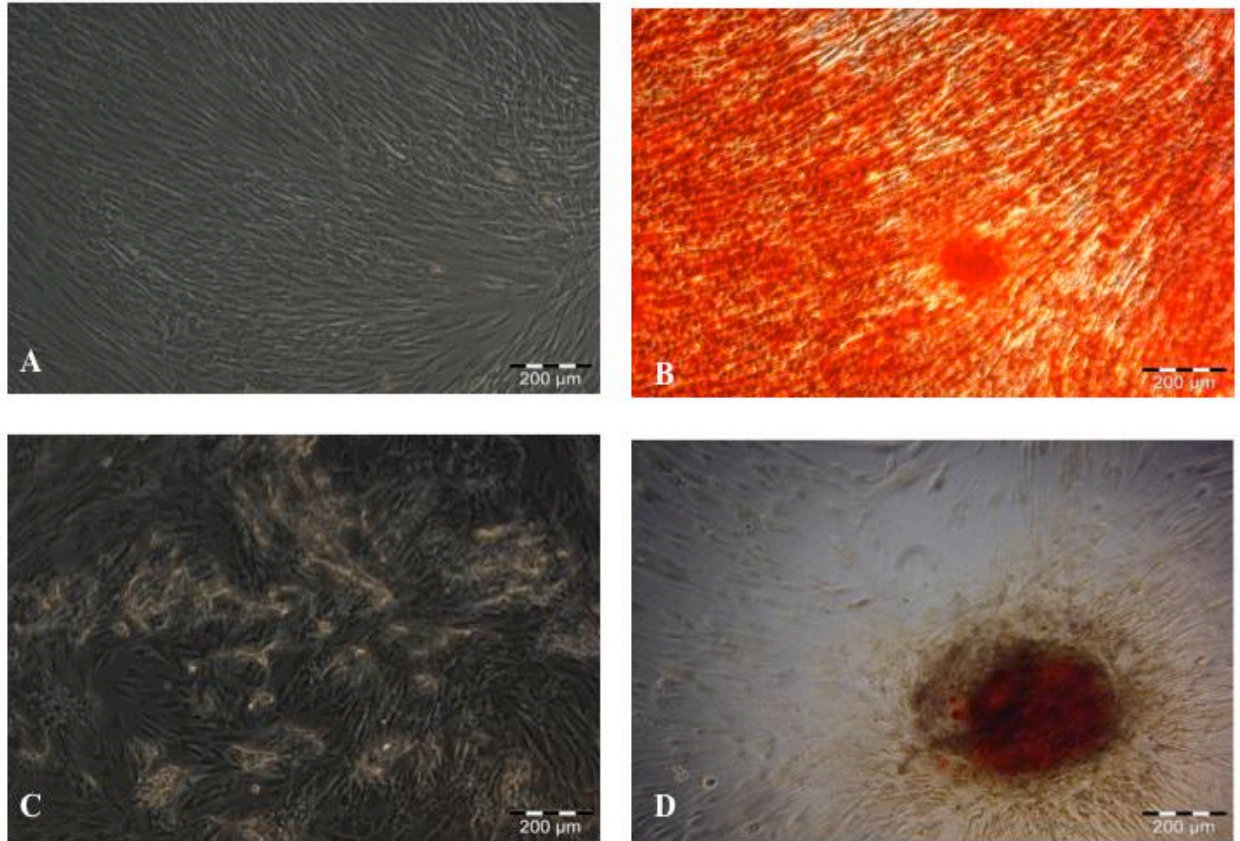


Figure 3.6.2: Alizarin Red Stains of monolayer and encapsulated HGMSCs. HGMSCs as monolayer culture (2D) and cells encapsulated in PuraMatrix™ (3-D). The morphology of differentiated cells A) Cells in monolayer in osteogenic medium at week 4 B) Cells induced with OM for 4 weeks and stained with Alizarin Red – orange color indicates calcium deposition C) Cells in PuraMatrix™ in OM (clustering of cells can be observed) F) 4 weeks -Cells in PuraMatrix™ were stained with Alizarin Red to detect the mineral deposit, presence of mineral deposition is observed for cells with in PuraMatrix™ gel.

3.7 HGMSCs seeded PuraMatrix™ induces *in vivo* bone formation

3.7.1 CT scans

CT scans show that at 2 and 4 weeks after subcutaneous implantation of HGMSCs seeded PuraMatrix™ scaffolds, clusters of radiopacities form at surgical sites (3.7.1A-F). The radiopacities suggest that the scaffold system combination has developed ectopic bone formation. In the volumetric representation, distinct nodules can be visualized on

experimental sides. Using the i-CAT software, cross sections of experimental and control side were observed and relative surface area was quantified. Cross section of the control side showed normal tissue whereas the experimental side showed radiopacities suggesting osteoid formation (Table 3.7.1).

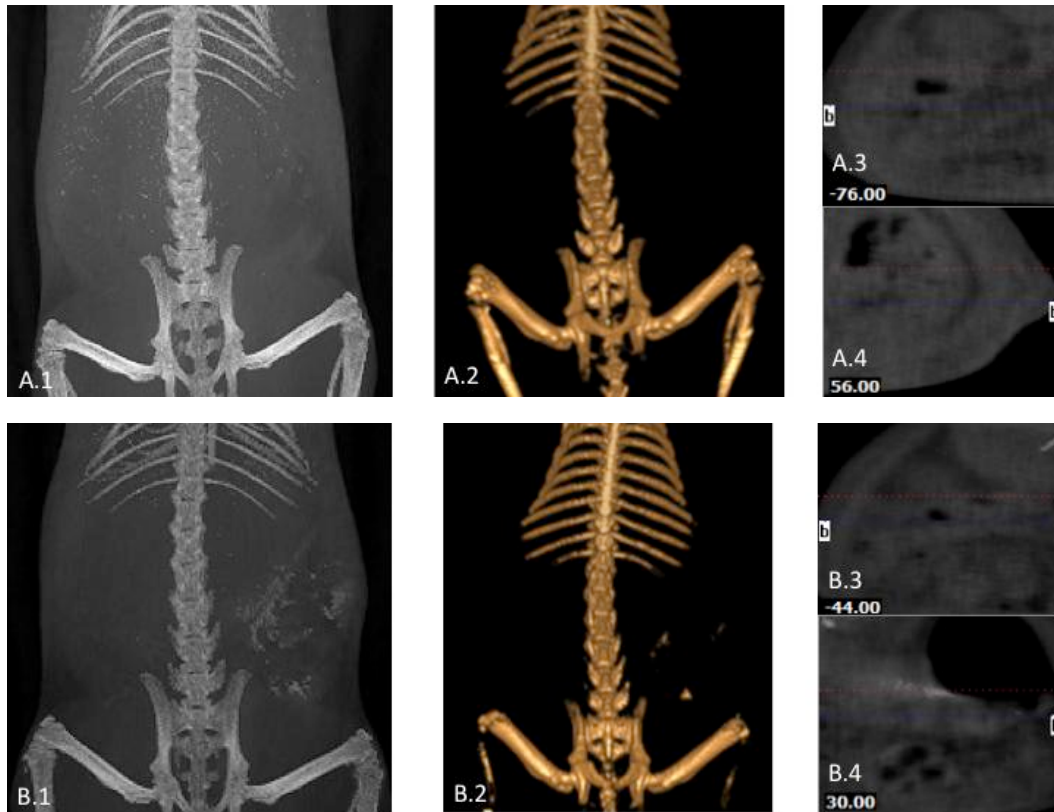


Figure 3.7.1A: CT Scans of Control and Week 2. Series of images from CT Scan of rat subject post surgery using i-CAT vision software showing 2D scans, 3D scans, and control and experiment cross sectional slices. A) CT scans of control rat shows no radiopacity at week 4. B) Shows 2 week CT scan of rats showing radiopacities starting to form.

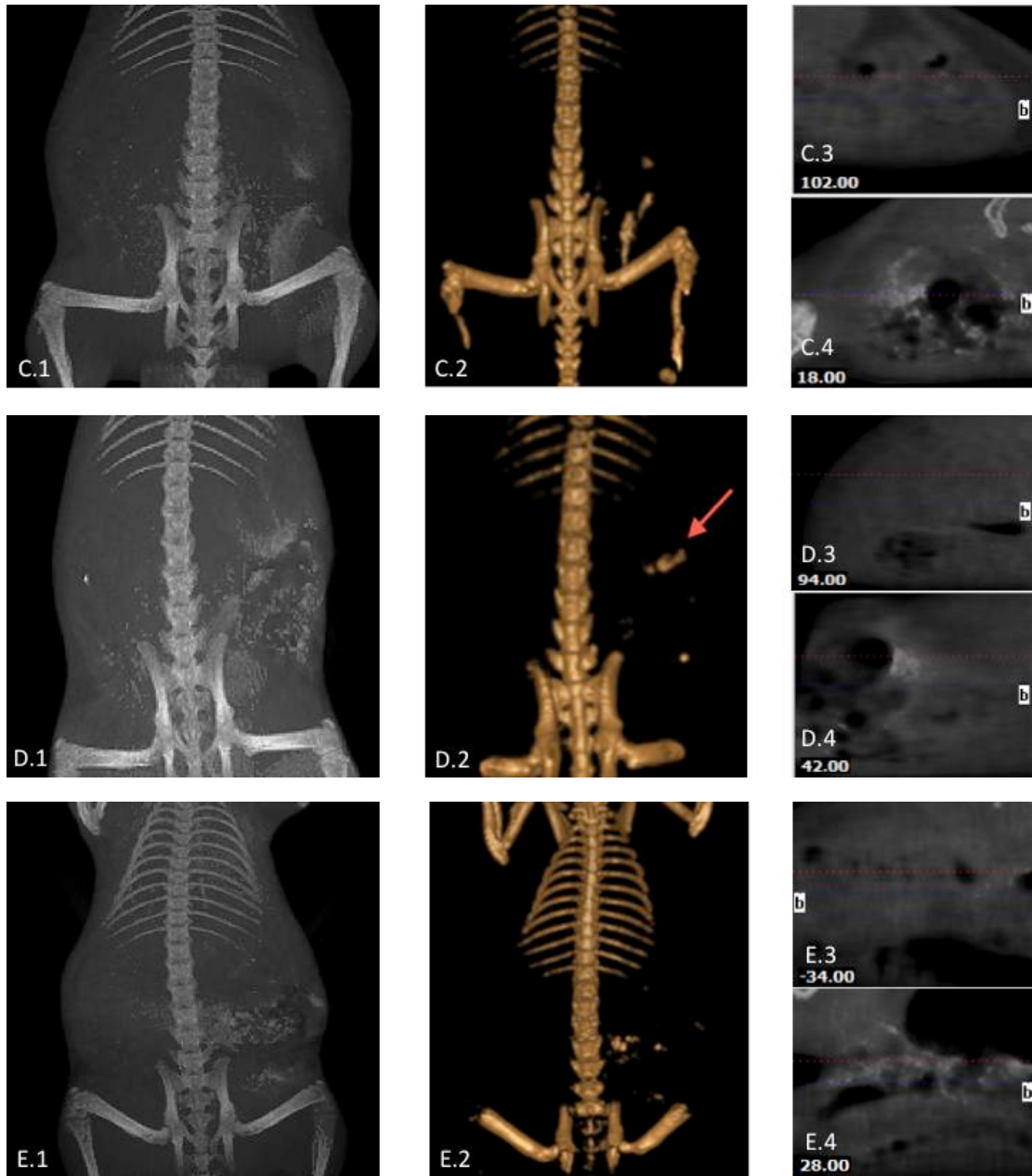


Figure 3.7.1B: CT Scans of week 4. CT scans of rats at 4 weeks time period.



Figure 3.7.1C: CT Scans of week 4. F.1) Significant clusters of radiopacities seen in 2D. F.2) Large radiopacity in experimental side suggesting bone formation F.3) Control cross-section shows no radiopacities F.4) Cross sectional slice of suspected bone shows radiopacity for quantitative measurements.

Number positive for radiopacity/total number of implants		
	Non-seeded PuraMatrix™	HGMScs Seeded PuraMatrix™
Control 1	0/6	
Preformed 1	0/3	1/3
Preformed 2	0/3	2/3
Injectable 1	0/3	2/3
Injectable 2	0/3	3/3
Injectable 3	0/3	3/3
Total	0/21	9/15
% per group	0	0.75

Table 3.7.1A: Radiographic findings. Number of radiopacities observed in control and experimental sides.

	Preformed		Injectable	
	PuraMatrix™	HGMSCs + PuraMatrix™	PuraMatrix™	HGMSCs + PuraMatrix™
Cross Sectional Area (pixels)	22,760 ± 2,233	20,983 ± 785	19,735 ± 2899	21,384 ± 870
Area of radiopacity, new bone formation (Pixels)	0	1,497 ± 1489	0	1,705 ± 915
Extent of new bone formation (%)	0	6.9 ± 6.9	0	9.2 ± 6

Table 3.7.1B: Percentage of radiopacity from CT Scans. Comparison of extent of new bone formation of HGMSCs seeded PuraMatrix™ compared to PuraMatrix™ scaffold only, which demonstrates evidence of bone formation.

3.7.2 Histological analysis

Histological analysis shows that 4 weeks after subcutaneous implantation of HGMSCs seeded PuraMatrix™ scaffolds, bone formation was present at surgical sites. Using the CT scans of radiopaque areas as a guide, tissue samples were surgically removed for analysis. There were no signs of infected wound, pus formation, skin necrosis, or dead rats during postoperative follow-up observations of the rat. This shows that the hydrogel scaffold is biocompatible with the animal and non-toxic. In the histological slides, tissue samples of the control side only show connective tissue showing that hydrogel was biodegradable. However, in one slide of the control side, a remnant of PuraMatrix™ scaffolds is observed (Figure 3.7.2A). In the H&E stained histological slides of the experimental sides, bone tissue can be observed with presence of osteoblasts (Figure 3.7.2B). Using Image-J software, area of bone tissue can be calculated relative to the

histological slide. Of the samples, the area of bone formation is present relative to the tissue sample size is 15%. Together with the radiographic observations, the data supported that the subcutaneous implantations of HGMSCs cells have formed osteoids with osteoblasts in PuraMatrix™ hydrogel.



Figure 3.7.2A: Recovery of scaffold implant. A.1) Vascularity observed formed subcutaneously indicating ectopic angiogenesis. A.2) Bone-like nodule observed. A.3) Nodule measured to 2mm and processed for histological analysis.

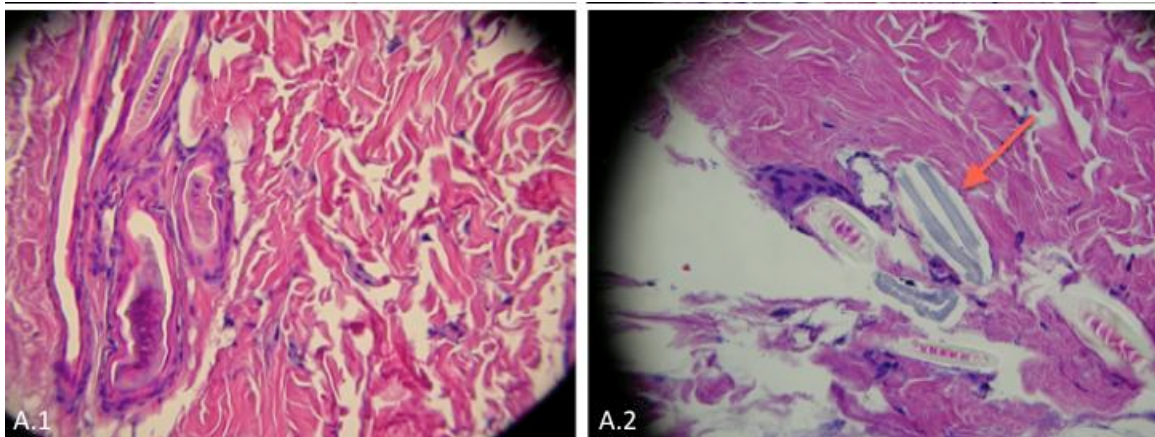


Figure 3.7.2B: Histological slides of control sites. Histological slides at 400x. A.1) Tissue sample of control side showing connective tissue only. A.2) Tissue sample of control side showing presence of remnants of PuraMatrix™ scaffold with no inflammatory cells or response.

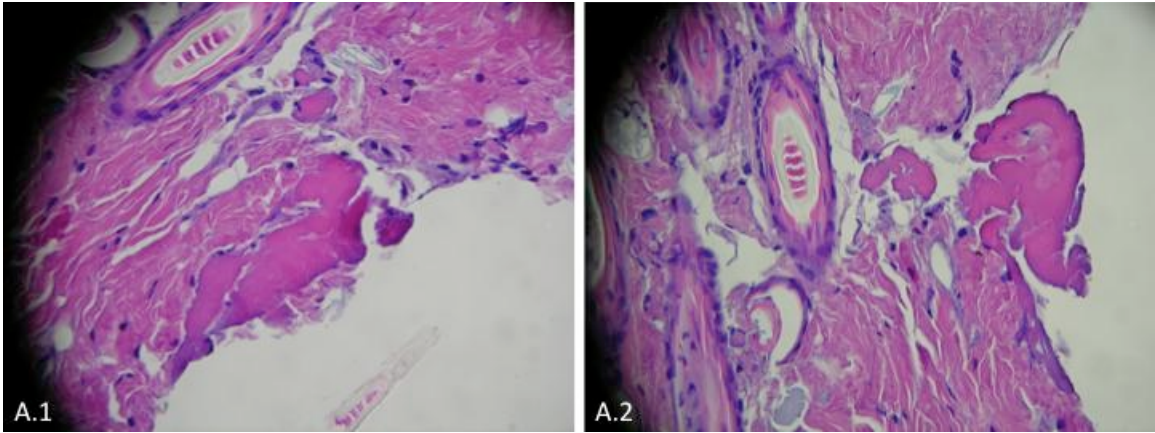


Figure 3.7.2C: Histological slides of experiment sites. A.1-A.2) Osteoid formation with osteoblasts at 400x.

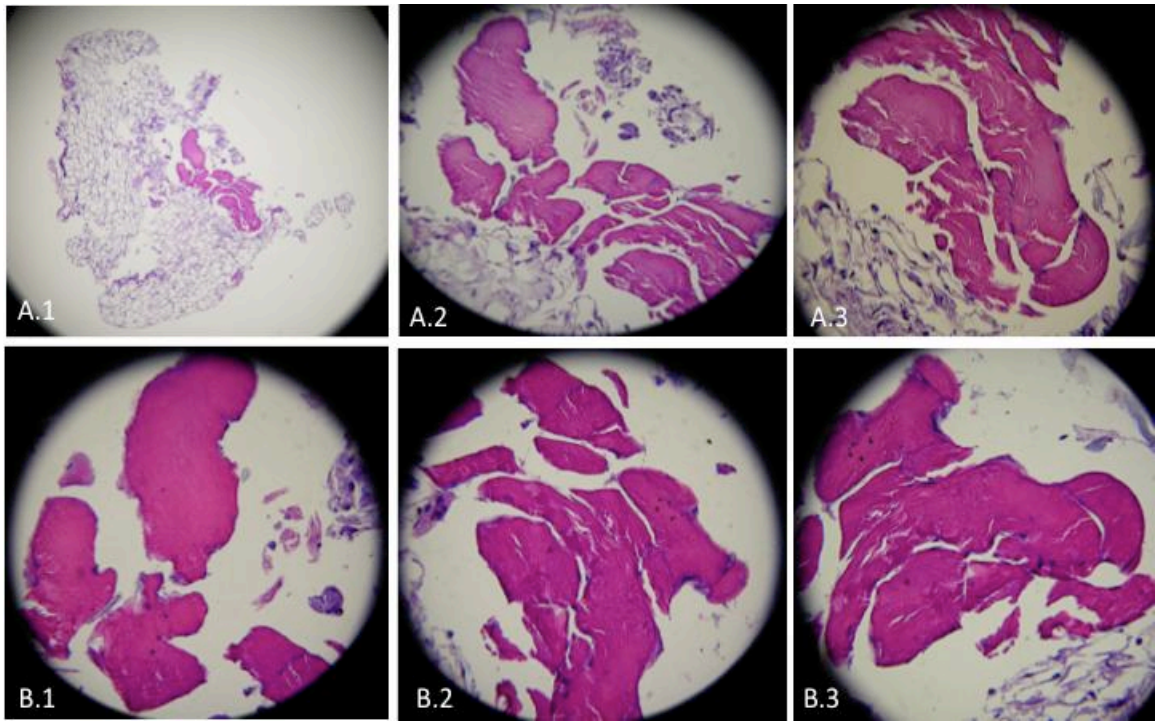


Figure 3.7.2D: Histological slides of experiment sites. A.1) Histological slide of osteoid formation at 100x. A.2 and A.3) Osteoid formation with osteoblasts present at edges. B.1-B.3) Osteoid formation seen at 630X showing presence of osteoblasts.

Number positive for bone formation/total number of implants		
	Non-seeded PuraMatrix™	HGMSCs Seeded PuraMatrix™
Control 1	0/6	
Preformed 1	0/3	0/3
Preformed 2	0/3	1/3
Injectable 1	0/3	1/3
Injectable 2	0/3	1/3
Injectable 3	0/3	0/3
Total	0/21	3/15
% per group	0	0.20

Table 3.7.2A: Recovered implants. Number of scaffold explants recovered from surgery in control and experimental sides.

	PuraMatrix™ Only	HGMSCs seeded PuraMatrix™
Tissue Sample Area (pixels)	1,787,140	2,878,668 ± 2,089,802
Area of new bone formation (Pixels)	0	354,376 ± 245,774
Extent of new bone formation (%)	0	12 ± 5.5

Table 3.7.2B: Percentage of bone formation from histological analysis. Comparison of extent of new bone formation of HGMSCs seeded PuraMatrix™ compared to PuraMatrix™ scaffold only, which demonstrates evidence of bone formation.

CHAPTER 4: CONCLUSION AND DISCUSSION

4.1 Discussion

Tissue engineering involves repair and regeneration of tissue using appropriate cell sources and optimal culture conditions and biodegradable scaffold. Developing an appropriate cell- scaffold system is the key success in [14] regeneration of bone tissue. Additionally, special consideration needs to be taken for pediatric tissue engineering applications, to meet the developmental changes in the children [14, 16]. The unique challenge in engineering craniofacial bone tissue for pediatric population is the ability to recapitulate the corresponding craniofacial developmental events and needs. Therefore, with regards to cleft lip and palate children, our long-term goal is to enhance bone formation in the region of hard palate and retain proper maxillofacial growth for the repair of cleft palate through an appropriate use of stem cells and scaffold systems.

In this study we have chosen HGMSCs as cell source. HGMSCs has highly proliferative and can be obtained from discarded tissue with less invasive manner. Furthermore, 90% of HGMSCs is derived from cranial neural crest cells [19, 20, 35], which are considered to be important for craniofacial development. Deficiency of neural crest cells may lead to the craniofacial developmental defects such as cleft lip and palate. Thus, HGMSCs present an appropriate stem cell source for the repair and regeneration of bone in craniofacial defects. Additionally, HGMSCs are capable of immunomodulatory functions and anti-inflammatory function [34] suggesting that they can be useful for faster healing and reduction of scar tissue formation.

The second component in bone tissue engineering is selecting a scaffold material. A suitable biological scaffold can create a microenvironment niche for a given cell type. The main objective of the study was to develop a novel composite cell- scaffold system for formation of bone. PuraMatrix™ is a biologically inspired peptide hydrogel scaffold that can be used to create tailored 3- dimensional micro-environment with the ability to self-assemble in biological environments from injectable application due to it's low viscosity [26, 27, 34]. Liquid as a starting material has advantageous that it can fill irregular shape of the defects such as cleft palate. This self-assemble peptide has nanofiber structure that enables the cells to adhere and proliferate the scaffold. PuraMatrix™ has been investigated for many tissue engineering applications, however with limited focus on bone regeneration [26, 58]. Table 4.1 shows the use of PuraMatrix™ in various *in vitro* and *in vivo* studies. In this study the novel combination of a self-assembled nanofibrous PuraMatrix™ – HGMSCs composite scaffold was characterized and bone formation ability was investigated in a subcutaneous implantation model within rat.

Literature Review of Current PuraMatrix™ Studies				
Author	Year	Article	Cells Used	Remarks
Ross V et al	2014	Dental pulp tissue engineering in full-length human root canals	Stem cells from exfoliated deciduous teeth	SHED differentiated into functional odontoblast
Cavalcanti B et al	2013	A hydrogel scaffold that maintains viability and supports differentiation of dental pulp stem cells.	Dental pulp stem cells	PuraMatrix™ and expressed markers of odontoblastic markers.
Moradi, F et al	2012	BD PuraMatrix™ peptide hydrogel as a culture system for human fetal schwann cells in spinal cord regeneration	Fetal Schwann Cells	Used for spinal injury in animal.
Henrisksson H.B. et al	2011	Investigation of different cell types and gel carriers for cell-based intervertebral disc therapy, <i>in vitro</i> and <i>in vivo</i> studies.	Human Mesenchymal Stem Cells, IVD cells, Chondrocytes	Useful for human degenerated intervertebral discs.
Kohgo T et al	2011	Bone regeneration with self-assembling peptide nanofiber scaffolds in tissue engineering for osseointegration of dental implants.	Dog Mesenchymal Stem Cells + Platelet-Rich Plasma	Bone regeneration around dental implants.
McGrath A et al	2010	BD PuraMatrix™ peptide hydrogel seeded with Schwann cells for peripheral nerve regeneration.	Schwann cells	Increased the rate of axonal regeneration across nerve defect.
Nakahara H et al	2010	Bone repair using a hybrid scaffold of self-assembling peptide PuraMatrix™ and polyetheretherketone cage in rats.	None	Bone regeneration was observed when they were used PEEK cages
Ortinou S et al	2010	Effect of 3D scaffold formation on differentiation and survival in human neural progenitor cells.	Human fetal neural progenitor cell	Neuronal differentiation of human neural progenitor cells has been reported.
Maher S et al	2009	A nanofibrous cell-seeded hydrogel promotes integration in a cartilage gap model	Chondrocytes	Cell-seeded TGF-B3 hydrogel can encourage cartilage integration
Yamaoka H et al	2006	Cartilage tissue engineering using human auricular chondrocytes embedded in different hydrogel materials.	Human auricular chondrocytes	Cartilage regeneration has been observed.
Bokhari M et al	2005	The enhancement of osteoblast growth and differentiation <i>in vitro</i> on a peptide hydrogel-polyHIPE polymer hybrid material	Rat osteoblasts	RAD16-I, PuraMatrix™, enhances osteoblast differentiation and growth
Kisiday J et al	2002	Self-assembling peptide hydrogel fosters chondrocyte extracellular matrix production and cell division: implications for cartilage tissue repair.	Chondrocytes	Cartilage like structure was formed

Table 4: Literature review of current PuraMatrix™ studies

In all our studies the cells cultured up to 3rd passage were used. In terms of mechanical stability 1% PuraMatrixTM was found to be mechanically stable, however our *in vitro* pilot studies encapsulated 0.5% PuraMatrixTM showed enhanced cell proliferation over 1% PuraMatrixTM. 0.5% PuraMatrixTM for all our *in vitro* studies and established the dose and time of cell delivery necessary for the *in vivo* studies.

The results of live/dead cell assay and WST demonstrated that cells are viable at all concentrations and the cell growth was observed till 7th after encapsulation. Over 90% of HGMSCs are viable and morphologically, cell growth was observed from day 1. At day 3rd cells attained spindle shaped. The high hydrophilic nature of the hydrogel and incorporation of Arg-Gly-Asp proteins or the RADA groups might have provided the cells to adhere and proliferate with in the gel. Higher water content raises the transport efficiency of nutrients into wastes out of the hydrogels [59]. Thus our *in vitro* studies demonstrated that PuramatrixTM was biocompatible. Additionally light microscopic observations and scanning electron microscope studies revealed that the nanofiber structures could assist the cells to attach and formed a micro environment similar to extracellular matrix [60]. It is interesting to note that the cells in the center appeared like spherical clusters when compared to the cells at the periphery. Our results confirmed that PuraMatrixTM induces osteogenic differentiation in the cells treated with osteogenic medium. The results of our study were in accordance with the previous reports [54].

In the *in vivo* study cells seeded scaffold systems were transplanted to subcutaneous sites via two delivery methods, implant method and injectable method using 0.5% PuraMatrix™ based on our *in vitro* data and previous studies. Nevertheless, the handling and implanting of preformed PuraMatrix™ to subcutaneous implantation was challenging, as the PuraMatrix™ would not retain its gelation form. However, the injectable delivery method poses significant ease in handling and delivery to subcutaneous sites in rats. Furthermore, we have chosen 500,000 (5×10^5) cells for implanting as the studies indicated that the cells implanted at density of 800,000 cells/ml of Dental pulp stem cells (DEPC) inhibited the growth [27] phase.

To visualize the extent of bone formation in subcutaneous sites on the dorsum of rats CT Scans were utilized. CT scans uses computer processed radiograph scans to produce tomographic images, or virtual slices. These cross-sectional images are used for diagnostic and therapeutic purposes in various medical settings in a non-invasive manner. Using the I-CAT software, the large series of two-dimensional radiographic images is generated to three-dimensional data to view scans in axial, coronal, or sagittal planes. This provides an advantage over traditional projection radiography, which only provides two-dimensional imagery. In studies using traditional projection radiography [58], only measurement in length can be reported. In studies using CT scans, 1-mm thick coronal sections can be produced from samples and scored for osseous repair/formation or outlined using ImageJ to present relative areas of bone per total volume [4, 8, 12, 22, 56]. CT scans do present with limitations as “stacking” of digital slices performs volumetric representation and can result in artifacts. In a study by Conjero, the data from CT scans

were not included in analysis because of insufficient resolution of films and states that quality of new bone growth was evaluated by gross, radiologic, and histological evaluation and quantitatively approximated. In more recent studies, microcomputed tomography scans have been more widely used in studies of this nature to quantify volume of interest (VOI) [12, 23, 61].

To confirm the radiographic findings, histological analysis were performed on PuraMatrix™ only and HGMSCs seeded PuraMatrix™ experiments. In our results, 3 sites out of 12 experimental subcutaneous implants yield gross visual bone formation. As stated, prior, the preformed delivery method posed a challenge and yield less results. Another difficulty was identifying and excising appropriate tissue samples for analysis. At 4 week time point, the CT scans served as a guide to approximate the location of subcutaneous implants but during the surgery, without gross presence of bone, identifying the tissue with osseous change or inflammatory changes proved challenging. However, with the histological sections of bone tissue that was obtained, surface area was calculated using Image J software and relative area of new bone was calculated.

In a recent study, Liao H et al in 2011 observed similar results to our studies implanting canine bone marrow derived mesenchymal stem cells in injectable thermo-responsive polymer hydrogel for 4 months [54]. This study observed similar *in vitro* results noting that MSCs in hydrogel showed better cell proliferation and improved osteogenic differentiation. The study observed ectopic bone formation using micro-CT analysis showing bone density mass in 2D axial and 3D view similar to the presentation in our

study. Also, osteoid formation with osteoblasts in bone matrix and positive mineralization were used with H&E stains, Manson's Trichrome stains, and von Kossa stains. This is also consistent with the osteoid formation also observed at week 4 in rat model in our study.

In other recent studies, Nguyen P et al in 2009 developed alveolar defect model in rat and observed bone formation using scaffold combo therapy [62, 63]. Similarly to our study, the proposed therapeutic goals were investigated by authors to develop a critical size defect in the alveolus of rats from incisors to zygomatic bone. With a suitable model established, the authors repaired the bony defects with different combinations of either absorbable collagen sponge or hydroxyapatite-tricalcium phosphate plus recombinant human bone morphogenetic protein-2 (rhBMP-2). Using micro-CT, new bone formation was observed in defects and seen in histological analysis. From the study, new bone formation plateaus at week 4 as macrophages and polymorphonuclear cells were present in disorganized array of fibroblasts and collagen with cuboidal-shaped osteoblasts observed depositing osteoid. This is consistent with our study as osteoid formation was observed at week 4 in our rat model. However, in comparison of histological findings, our osteoid formation had less prevalent osteoblast presence.

4.2 Conclusion

In conclusion, our *in vitro* studies demonstrate that the PuraMatrix™ hydrogel enhanced cell proliferation and osteogenic differentiation. The null hypothesis is rejected as our *in vivo* study demonstrated the presence of osteoid like structures at week 4 when PuraMatrix™ hydrogel was injected with osteo-induced HGMSCs in ectopic bone formation rat model.

Further research will need to be completed to develop a reproducible protocol and model in subcutaneous implantation and will investigate the potential of HGMSCs seeded PuraMatrix™ combination for the repair of critical size defects in hard palate of rats.

APPENDIX

Number positive for radiopacity/total number of implants		
	Non-seeded PuraMatrix™	HGMScs Seeded PuraMatrix™
Control 1	0/6	
Preformed 1	0/3	1/3
Preformed 2	0/3	2/3
Injectable 1	0/3	2/3
Injectable 2	0/3	3/3
Injectable 3	0/3	3/3
Total	0/21	9/15
% per group	0	0.75

Relative surface area of radiopacities			
	Total Surface area (pixels)	Radiopacity area (pixels)	Percent (%)
CO1	0	0	0
CP1	22130	2614	15.5
CP31	21539	444	2
PR11	20428	2550	11.18
SQ2	20428	1719	8.4
SQ3	21596	784	3.6
N	5	5	5
Mean	21224.2	1622.2	8.26
STDEV	762.5	993	5.6

Number positive for bone formation/total number of implants		
	Non-seeded PuraMatrix™	HGMScs Seeded PuraMatrix™
Control 1	0/6	
Preformed 1	0/3	0/3
Preformed 2	0/3	1/3
Injectable 1	0/3	1/3
Injectable 2	0/3	1/3
Injectable 3	0/3	0/3
Total	0/21	3/15
% per group	0	0.20

Surface Area of Histological Slides			
	Total Surface Area (pixels)	Bone Surface Area (pixels)	Percent (%)
5222	5038848	492174	9.8
5228	2729973	500335	18.3
5330	867185	70619	8
N	5	5	5
Mean	21224.2	1622.2	8.26
STDEV	762.5	993	5.6

BIBLIOGRAPHY

1. Meng, L., *Biological mechanisms in palatogenesis and cleft palate* Journal of Dental Research, 2009. **88**(1): p. 22-33.
2. Moreau, J., *Tissue engineering solutions for cleft palates*. Journal of Oral Maxillofacial Surgery, 2007: p. 2503-2511.
3. Marazita, M., *Current Concepts in the embryology and genetics of cleft lip and cleft palate*. Clinics in Plastic Surgery, 2004. **31**: p. 125-140.
4. Conejero, A., *Repair of palatal bone defects using osteogenically differentiated fat-derived stem cells*. Plastic and Reconstructive Surgery, 2006: p. 857-863.
5. Conejero, J.A., *Repair of Palatal Bone Defects Using Osteogenically Differentiated Fat-Derived Stem Cells*. Plastic and Reconstructive Surgery, 2006. **117**.
6. Greenwald, A.S., *Bone-graft substitutes: facts, fictions and applications*. The journal of bone and joint surgery, 2001. **83**: p. 98-103.
7. Morselli, P.G., *Treatment of alveolar cleft performing a pyramidal pocket and an autologous bone grafting* The Journal of Craniofacial Surgery, 2009. **20**(5): p. 1566-1570.
8. Behnia, H., *Secondary repair of alveolar clefts using human mesenchymal stem cells* 2009. **108**: p. e1-e6.
9. Kang, E.-J., *In vitro and in vivo osteogenesis of porcine skin-derived mesenchymal stem cell-like cells with a demineralized bone and fibrin glue scaffold* Tissue Engineering, 2010. **16**(3): p. 815-827.
10. Vargel, I., *Solven-dehydrated calvarial allografts in craniofacial surgery* Plastic Reconstructive Surgery, 2004. **114**: p. 298-306.
11. Clokie, C.M., et al., *Closure of critical sized defects with allogenic and alloplastic bone substitutes*. J Craniofac Surg, 2002. **13**(1): p. 111-21; discussion 122-3.
12. Liu, G., *Evaluation of partially demineralized osteoporotic cancellous bone matrix combined with human bone marrow stromal cells for tissue engineering: an in vitro and in vivo study*. Calcif Tissue Int, 2008. **83**: p. 176-185.
13. GP, R., *Cancellous allograft versus autologous bone grafting for repair of comminuted distal radius fractures: a prospective, randomized trial*. Journal of Trauma, 2006. **60**: p. 1322-1329.

14. Patel, M., *Biomaterial Scaffolds in Pediatric Tissue Engineering*. Pediatric Research, 2008. **63**: p. 497-501.
15. Zuk, P., *Tissue engineering craniofacial defects with adult stem cells? Are we ready yet?* Pediatric Research, 2008. **63**(5): p. 478-486.
16. Mao, J., *Craniofacial tissue engineering by stem cells* Journal of Dental Research, 2006. **85**(11): p. 966-979.
17. Tomar, G.B., *Human gingiva-derived mesenchymal stem cells are superior to bone marrow-derived mesenchymal stem cells for cell therapy in regenerative medicine* Biochemical and Biophysical Research Communications, 2010. **393**: p. 377-383.
18. Carstanjen, B., *Successful engraftment of cultured autologous mesenchymal stem cells in a surgically repaired soft palate defect in an adult horse*. The Canadian Journal of Veterinary Research, 2006: p. 143-147.
19. Xu, X., *Gingivae contain neural-crest and mesoderm-derived mesenchymal stem cells* Journal of Dental Research, 2013: p. 1-8.
20. Zhang, Q., *Mesenchymal stem cells derived from human gingiva are capable of immunomodulatory functions and ameliorate inflammation-related tissue destruction in experimental colitis*. Journal of Immunology, 2009. **183**: p. 7787-7798.
21. Tamer, M., *Progenitor and stem cells for bone and cartilage regeneration* Journal of Tissue Engineering and Regenerative Medicine, 2009. **3**: p. 327-337.
22. Por, Y.-C., *Bone generation in the reconstruction of a critical size calvarial defect in an experimental model* Journal of Craniofacial Surgery, 2007. **36**(11): p. 911-919.
23. Patel, Z.S., *Dual Delivery of an angiogenic and an osteogenic growth factor for bone regeneration in a critical size defect model* Bone, 2008. **43**(5): p. 931-940.
24. Lee, K.Y., *Hydrogels for Tissue Engineering* Chemical Reviews, 2001. **101**(7): p. 1869-1879.
25. Park, J.-B., *The use of hydrogels in bone-tissue engineering* Biomaterials and Bioengineering in Dentistry, 2011. **16**(1): p. e115-118.
26. Bokhari, M., *The enhancement of osteoblast growth and differentiation in vitro on a peptide hydrogel - polyHIPE polymer hybrid material* Journal of Biomaterials 2005. **26**: p. 5198-5208.

27. Cavalcanti, B., *A hydrogel scaffold that maintains viability and supports differentiation of dental pulp stem cells*. Journal of dental Materials 2013. **29**: p. 97-102.
28. Khademhosseini, A., *Microengineered hydrogels for tissue engineering* Journal of Biomaterials, 2007. **28**: p. 5087-5092.
29. Van-Den-Dolder, J., *Platelet-rich plasma: Quantification of growth factor levels and the effect on growth and differentiation of rat bone marrow cells* Tissue Engineering, 2006. **12**(11): p. 3067-3073.
30. Zhao, L., *An injectable calcium phosphate-alginate hydrogel-umbilical cord mesenchymal stem cell paste for bone tissue engineering*. Biomaterials, 2010. **31**: p. 6502-6510.
31. Seo, B., *SHED repair critical-size calvarial defects in mice*. Oral Diseases, 2008. **14**: p. 428-434.
32. Sakai, V.T., *Tooth slice/scaffold model of dental pulp tissue engineering* Advance Dental Research, 2011. **23**(3): p. 325-332.
33. Zhang, Q., *Human oral mucosa and gingiva: a unique reservoir for mesenchymal stem cells*. Journal of Dental Research, 2012.
34. Zhang, S., *PuraMatrix: Self-assembling Peptide nanofiber Scaffolds*, in *Scaffolding in Tissue Engineering*. Cambridge, MA.
35. Pittenger, M., *Multilineage potential of adult human mesenchymal stem cells*. Science, 1999. **284**(5411): p. 143-147.
36. Chung, I-h., *Stem cell property of postmigratory cranial neural crest cells and their utility in alveolar bone regeneration and tooth development*. Stem Cells, 2009. **27**(4): p. 866-877.
37. Misawa, H., et al., *PuraMatrix facilitates bone regeneration in bone defects of calvaria in mice*. Cell Transplant, 2006. **15**(10): p. 903-10.
38. Moradi, F., *BD PuraMatrix Peptide Hydrogel as a Culture System for Human Fetal Schwann Cells in Spinal Cord Regeneration* Journal of Neuroscience Research, 2012. **90**: p. 2335-2348.
39. Naotaka Kishimoto, Y.M., Ryoichi Mori, Yoshiya Hashimoto, Koichi Imai, Takeshi Omasa, Junichiro Kotani, *Bone Regeneration Using Dedifferentiated Fat Cells with PuraMatrix*. J Oral Tissue Engin, 2008. **6**(2): p. 127-134.

40. Abu-Yousif, A., *PuraMatrix encapsulation of cancer cells*. Journal of Visualized Experiments, 2009. **34**.
41. McGrath, A., *BD PuraMatrix peptide hydrogel seeded with Schwann cells for peripheral nerve regeneration*. Brain Research Bulletin 2010. **83**: p. 207-213.
42. Maher, S., *A nanofibrous cell-seeded hydrogel promotes integration in a cartilage gap model* Journal of Tissue Engineering and Regenerative Medicine, 2009. **4**: p. 25-29.
43. Gelain, F., *Designer self-assembling peptide nanofiber scaffolds for adult mouse neural stem cell 3-dimensional cultures*. PLoS One, 2006. **1**: p. e119.
44. Kisiday, J., *Self-assembling peptide hydrogel fosters chondrocyte extracellular matrix production and cell division: Implications for cartilage tissue repair*. Proceedings of the National Academy of Sciences of the United States of America, 2002. **99**(15): p. 9996-10001.
45. Ortinau, S., *Effect of 3D-scaffold formation on differentiation and survival in human neural progenitor cells*. BioMedical Engineering Online, 2010. **9**(70).
46. V, R., *Dental Pulp Tissue Engineering in Full-length Human Root Canals*. Journal of Dental Research, 2013. **92**(11): p. 970-975.
47. Yamaoka, H., *Cartilage tissue engineering using human auricular chondrocytes embedded in different hydrogel materials*. Journal of Biomedical Materials Research 2006.
48. Fawzy El-Sayed, K.M., et al., *Periodontal regeneration employing gingival margin-derived stem/progenitor cells: an animal study*. J Clin Periodontol, 2012. **39**(9): p. 861-70.
49. Henriksson, H., *Investigation of different cell types and gel carriers for cell-based intervertebral disc therapy, in vitro and in vivo studies* Journal of Tissue Engineering and Regenerative Medicine, 2011. **6**(9).
50. Furlaneto, F., *Bone healing in critical-size defects treated with bioactive glass/calcium sulfate: a histologic and histometric study in rat calvaria*. . Clinical Oral Implant Research, 2007: p. 1-8.
51. Whang, K., *Ectopic bone formation via rhBMP-2 delivery from porous bioabsorbable polymer scaffolds*. Journal of Biomedical Materials Research, 1998: p. 491-499.

52. Meno-Tetan, G.M., *Physiologically based pharmacokinetic modeling of FTY720 (2-amino-2[2-(-4-octylphenyl)ethyl]propane-1,3-diol hydrochloride) in rats after oral and intravenous doses*. Drug Metabolism and Disposition 2006. **34**: p. 1480-1487.
53. Hosseinkhani, H., *Bone regeneration on a collagen sponge self-assembled peptide-amphiphile nanofiber hybrid scaffold*. Tissue Engineering, 2007. **13**(1): p. 11-19.
54. Liao, H.-T., *Osteogenic differentiation and ectopic bone formation of canine bone marrow-derived mesenchymal stem cells in injectable thermo-responsive polymer hydrogel* Tissue Engineering, 2011. **Part C**: p. 1139-1149.
55. Ludlow, J., *Dosimetry of two extraoral direct digital imaging devices: NewTom cone beam CT and Orthophos Plus DS panoramic unit*. Dentomaxillofacial Radiology, 2003. **32**: p. 229-234.
56. Patel, M., *Cyclic acetal hydroxyapatite nanocomposites for orbital bone regeneration*. Tissue Engineering, 2010. **16**: p. 55-65.
57. Clark, G., *Staining procedures*. 4th ed. 1981, Baltimore, MD: Williams and Wilkins.
58. Nakahara, H., *Bone repair using a hybrid scaffold of self-assembling peptide PuraMatrix and Polyetheretherketone cage in rats*. Cell Transplantation, 2010. **19**: p. 791-797.
59. Drury, J.a.M., *Hydrogels for tissue engineering scaffold design variables and applications*. Biomaterials, 2003. **24**(24): p. 4337-4351.
60. Zhang, S., *Designer self-assembling peptide nanofiber scaffolds for 3D tissue cell cultures*. Seminars in Cancer Biology, 2005. **15**: p. 413-420.
61. Stephan, S.J., *Injectable tissue-engineered bone repair of a rat calvarial defect* Laryngoscope, 2010. **120**: p. 895-901.
62. Nguyen, P., *Establishment of a critical-sized alveolar defect in the rat: a model for human gingivoperiosteoplasty*. Plastic and Reconstructive Surgery, 2009. **123**: p. 817-825.
63. Nguyen, P., *Scaffold-based rhBMP-2 therapy in a rat alveolar defect model: Implications for human gingivoperiosteoplasty*. Plastic and Reconstructive Surgery, 2009. **124**: p. 1829-1839.